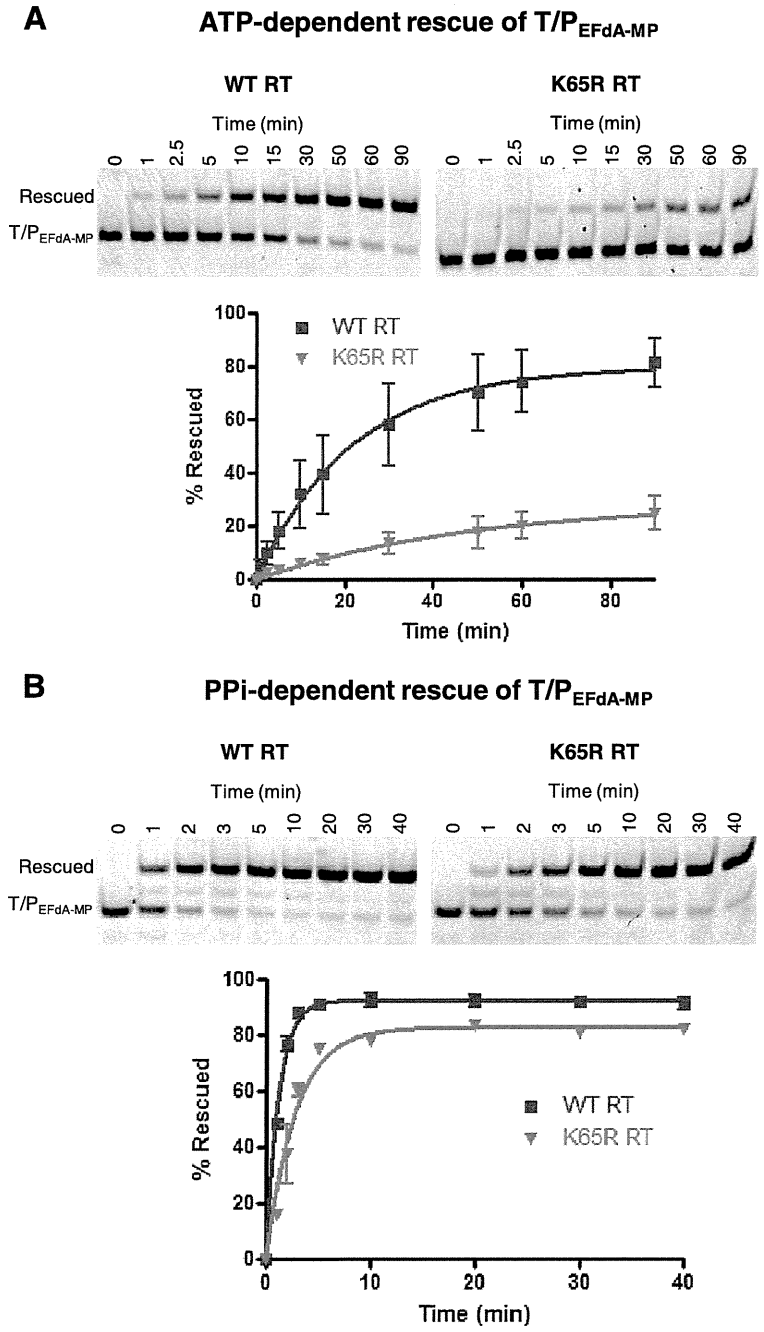

Figure 3 ATP- and PPi-dependent rescue of EFdA-MP terminated primers by WT and K65R RTs. (**A**) ATP-dependent rescue of $T_{d31}/P_{d18\text{-}P0\text{-}EFdA\text{-}MP}$. Purified $T_{d31}/P_{d18\text{-}P0\text{-}EFdA\text{-}MP}$ was incubated with WT or K65R RT in the presence of 10 mM $MgCl_2$, 3.5 mM ATP, 100 μM dATP, 0.5 μM dTTP, and 10 μM ddGTP at 37°C. Aliquots of the reaction were stopped at the indicated time points (0–90 min). The results of at four independent experiments were plotted using one site hyperbola in Graphpad Prism 4. (**B**) PPi-dependent rescue of $T_{d31}/P_{d18\text{-}P0\text{-}EFdA\text{-}MP}$. Purified $T_{d31}/P_{d18\text{-}P0\text{-}EFdA\text{-}MP}$ was incubated with WT or K65R RT in the presence of 6 mM $MgCl_2$, 150 μM PPi, 100 μM dATP, 0.5 μM dTTP, and 10 μM ddGTP at 37°C. Aliquots of the reaction were stopped at the indicated time points (0–40 min). The results of two independent experiments were plotted using one site hyperbola in Graphpad Prism 4.

as HIV therapeutics. The clinical cut-off for tenofovir resistance is defined as a 2.1-fold reduction in virological response. It is associated with the presence of the tenofovir-resistance signature mutation K65R in the reverse transcriptase gene [50]. We report here that EFdA is highly potent against tenofovir-resistant K65R HIV, and inhibits this mutant 2.5-fold *more* efficiently than WT HIV. Given the fact that clinical resistance to tenofovir is considered a 2.1-fold decrease

in susceptibility, we consider a 2-fold increase in susceptibility as significant hypersusceptibility. Understanding the mechanism by which HIV becomes resistant or more susceptible to EFdA could allow us to overcome drug resistance challenges and improve the current combination therapies. We have previously demonstrated that EFdA is highly efficient in suppressing viral replication of clinical isolates harboring signature mutations to other NRTIs and NNRTIs, including isolates containing 3TC/FTC resistance mutation M184V; TAMs or Q151M complex mutations that confer resistance to AZT, d4T, and abacavir; and nevirapine and efavirenz resistance mutations K103N and Y181C [45]. In addition, we have recently shown that EFdA is 3 logs more potent in SIV inhibition than tenofovir, AZT, and 3TC, and EFdA treatment decreases viral load in SIV-infected macaques by 3–4 logs within 1 week of SIV therapy and eventually to non-detectable levels [51]. The present study demonstrates that the K65R tenofovir-resistance RT mutation confers HIV hypersensitivity to EFdA compared to WT HIV. Other studies have shown that NRTI resistance mutations can confer enhanced susceptibility to other NRTIs. Specifically, the K65R and to a lesser extent the L74V RT mutations have been reported to suppress AZT resistance [43,52-55]. In addition, we have previously reported that K65R and L74V HIVs can be hypersusceptible to NRTIs with 4'-ethynyl substitutions [45,56]. The NNRTI-resistance mutation Y181C also increases susceptibility to AZT [57,58]. Moreover, the 3TC/FTC-resistance mutation M184V also increases HIV sensitivity to AZT by decreasing the excision efficiency of AZT-MP [22,53,59-61]. Finally, we have recently shown that the 172K polymorphism can enhance susceptibility to both NRTIs and NNRTIs [62].

To determine whether the K65R RT mutation has the same effect at the enzyme level as well, we also carried out inhibitor susceptibility experiments with WT and K65R recombinant RT enzymes. Indeed, our enzymatic assays clearly showed that K65R RT is more susceptible to inhibition by EFdA-TP than WT RT. We thus focused on the biochemical mechanism of the enhanced EFdA susceptibility. We previously reported that EFdA is a TDRTI and inhibits primarily by blocking translocation after its incorporation at the 3'-end of the primer [45,46]. Hence, we investigated the effect of the K65R mutation on translocation using the site-specific Fe^{2+} footprinting assay. We found that K65R mutation has only a small effect on the translocation state of the EFdA-MP-terminated DNA·RT complex suggesting that the EFdA-MP-terminated primers stay at the nucleotide binding site (N site) of K65R RT as much as they do at the N site of WT RT. Since the EFdA resistance was not the result of changes in translocation efficiency, we hypothesized that K65R affects either the incorporation of the inhibitor itself, or its excision from EFdA-terminated primers. The effect on incorporation efficiency was assessed with single nucleotide incorporation experiments, whereas the effect on excision was measured in PPi- and ATP-dependent excision experiments under steady state conditions. Our results showed that the K65R mutation decreased the incorporation efficiencies of EFdA-TP and dATP to the same extent. Since pyrophosphorolysis is the reverse reaction of polymerization we hypothesized that it would also be slower in the presence of this mutation. This was confirmed by a PPi-based excision assay where we measured unblocking of EFdA-MP from the 3'-end of the primer. We found that K65R reduced excision and kept EFdA-MP-terminated primers blocked, explaining the hypersusceptibility that we have reported. In addition, when we used conditions that more closely mimic cell-based conditions, with ATP as the unblocking reagent and also all dNTPs present in the reaction to extend the unblocked primers, we also found that K65R reduced excision. Since the footprinting data did not show any significant difference in the translocation efficiency we can therefore conclude that the excision is not decreased because the EFdA-MP-terminated primers reside less at the excisable site. A decreased unblocking of EFdA-MP-terminated primers is not due to their inability to bind at the excisable N site of K65R RT. Instead, the molecular models in Figure 4 suggest that residues R65 and K65 interact differently with R72 and the phosphate moieties of EFdA-TP or dNTP, and thus may differentially affect the recognition of the pyrophosphate donor (ATP or PPi) and its nucleophilic attack on EFdA-terminated primers. Future crystallographic studies should provide more details on the molecular basis of excision-based EFdA resistance.

Conclusion

We have provided virological and biochemical data demonstrating that the K65R RT mutation confers enhanced sensitivity to EFdA. We reported here that the mechanism of hypersensitivity is mainly through reduced excision of the chain terminating EFdA-MP. Our findings demonstrated that EFdA is a very potent NRTI and it could be used not only against WT HIV but also against tenofovir-resistant HIVs. The primary resistance mutation for EFdA is M184V and combination with tenofovir could be similar to the pair of mutations for 3TC/AZT combination. Unlike AZT and 3TC which are analogs of different deoxynucleosides, EFdA and tenofovir are both deoxyadenosine analogs and would theoretically compete to each other. However, they are activated/phosphorylated by different pathways [45]. Therefore, combination of EFdA with tenofovir could help suppress K65R resistance. This conclusion has significant potential therapeutic implications. Moreover, EFdA would be a good candidate in salvage therapies for patients that fail tenofovir-treatment due to K65R resistance.

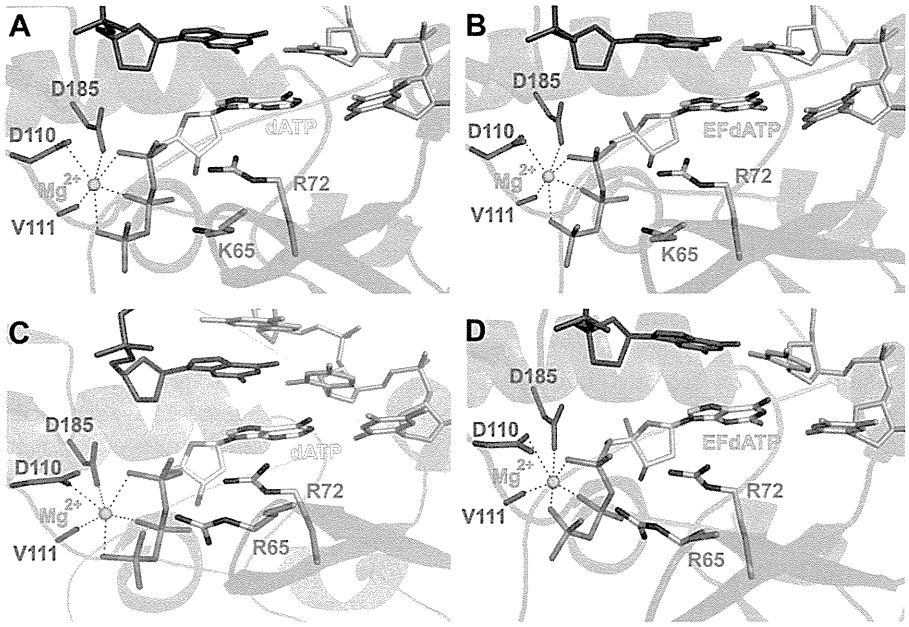

Figure 4 Molecular models of dATP and EFdA-TP in the active sites of WT and K65R HIV RT. dATP (yellow sticks, **A** and **C**) and EFdA-TP (cyan sticks, **B** and **D**) are shown at the active sites of WT HIV RT, (**A** and **B**) or K65R HIV RT (**C** and **D**). The fingers and palm subdomains are shown in blue and red cartoon, respectively. The primer and template strands are shown in dark gray and light gray sticks, respectively. Figures were made using PyMOL (The PyMOL Molecular Graphics System, Version 1.3 Schrödinger, LLC).

Methods

Cells and viruses

TZM-bl cells (CCR5 transduced HeLa-CD4/LTR-β-gal and luciferase cells) were obtained from the AIDS Research and Reference Reagent Program, the National Institutes of Health (NIH). 293T and TZM-bl cells were maintained in Dulbecco's Modified Eagle Medium supplemented with 10% fetal calf serum, 100 U/ml penicillin and 100 μg/ml streptomycin, and used for transfection and antiviral assays, respectively.

K65R RT mutation was introduced by site-directed mutagenesis as described previously [63,64]. Briefly, the desired mutations were introduced into the *Xma* I - *Nhe*I region (759 bp) of pTZNX1, which encodes nucleotides Gly-15 to Ala-267 of HIV-1 RT. After mutagenesis, the *Xma*I - *Nhe*I cassettes were inserted back into pNL101 and confirmed by sequencing. Viral stocks were obtained by transfection of each molecular clone into 293T cells using Fugene 6 (Roche, Mannheim, Germany), harvested and stored at −80°C until use.

Cell-based drug susceptibility assays

Single-replication-cycle drug susceptibility assays were performed in triplicates using TZM-bl cells. TZM-bl cells were infected with diluted virus stock at 400,000 relative light units (RLU) in the presence of increasing concentrations of RTIs and cultured for 48 h. The luciferase marker gene expressions were measured using the Bright-Glo (Promega, WI). Susceptibility to NRTIs was calculated as the concentration that reduces RLU (infection) by 50% (50% effective concentration [EC_{50}]). The data were obtained from the results of at least three independent experiments and the P values were determined using *t*-test statistical analysis.

Enzymes and nucleic acids

HIV-1 RTs were expressed in JM-109 (Invitrogen) bacteria and purified by nickel affinity chromatography and monoQ anion exchange chromatography as previously described [46,65-69]. Oligonucleotides used in this study were chemically synthesized and purchased from Integrated DNA Technologies (Coralville, IA). Sequences of the DNA substrates are shown in Table 3. Deoxynucleotide triphosphates and dideoxynucleotide triphosphates were purchased from Fermentas (Glen Burnie, MD). EFdA was synthesized by Yamasa Corporation (Chiba, Japan) as described before [70]. Using EFdA as starting material the triphosphate form EFdA-TP was synthesized by TriLink BioTechnologies (San Diego, CA). Concentrations of nucleotides and EFdA-TP were calculated spectrophotometrically on the basis of absorption at 260 nm and their extinction coefficients. All nucleotides were treated with inorganic pyrophosphatase (Roche Diagnostics) as described previously [26] to remove traces of PPi contamination that might interfere with the rescue assay.

Enzymatic drug susceptibility assays

Inhibition of HIV-1 RT-catalyzed DNA Synthesis by EFdA-TP

DNA template was annealed to 5'-Cy3 labeled DNA primer (3:1 molar ratio) ($T_{d31}/P_{d18\text{-}P0}$). To monitor primer extension, the DNA/DNA hybrid (20 nM) was incubated at 37°C with WT or K65R HIV-1 RT (20 nM) in a buffer containing 50 mM Tris (pH 7.8) and 50 mM NaCl (RT buffer). Subsequently, varying amounts of EFdA-TP were added and the reactions were initiated by the addition of 6 or 10 mM $MgCl_2$ in a final volume of 20 μl. All dNTPs were present at a final concentration of 1 μM in the presence or absence of 3.5 mM ATP. The reactions were terminated after 50 minutes by adding equal volume of 100% formamide containing traces of bromophenol blue. The products were resolved on 15% polyacrylamide 7 M urea gels. In this and in subsequent assays the gels were scanned with a Typhoon FLA 9000 PhosphorImager (GE Healthcare, NJ). The bands corresponding to fully-extended product were quantified using Multi Gauge software. The results of at least four independent experiments were plotted as percent full extension using one site-competition nonlinear regression in GraphPad Prism 4 to determine the mean and standard deviation of the IC_{50} for EFdA-TP.

Steady-state Kinetics

Single nucleotide incorporation of dATP and EFdA-TP by WT and K65R RTs

Steady-state kinetic parameters K_m and k_{cat} for incorporation of EFdA-TP or dATP were determined using single nucleotide incorporation in gel-based assays under saturating concentrations of T/P (10-fold excess over RT). Reactions were carried out in RT buffer, 6 mM $MgCl_2$, 100 nM $T_{d26}/P_{d18\text{-}P5}$ or $T_{d31}/P_{d18\text{-}P0}$ or T_{d31A}/P_{d21} (Table 3) and 10 nM WT or K65R HIV-1 RT in a final volume of 20 μl and stopped at indicated reaction times. The products were resolved and quantified as described above. K_m and k_{cat} were determined graphically using the Michaelis-Menten equation. Reactions were carried out in two to four independent experiments to determine the mean and standard deviation values.

Site-specific Fe^{2+} footprinting assay

Site-specific Fe^{2+} footprints were monitored on 5'-Cy3-labeled DNA templates. 100 nM of 5'-Cy3-T_{d43}/P_{d30} was incubated with 600 nM WT or K65R HIV-1 RT in a buffer containing 120 mM sodium cacodylate (pH 7), 20 mM NaCl, 6 mM $MgCl_2$, and 1 μM EFdA-TP, to allow quantitative chain-termination. Prior to the treatment with Fe^{2+}, complexes were pre-incubated for 7 min with increasing concentrations of the next incoming nucleotide (dTTP). The complexes were treated with ammonium iron sulfate (1 mM) as previously described [46,47]. This reaction relies on autoxidation of Fe^{2+} [71] to create a local concentration of hydroxyl radicals, which cleave the DNA at the nucleotide closest to the Fe^{2+} specifically bound to the RNase H active site. These experiments were performed at least twice.

ATP- and PPi-dependent excision and rescue of $T/P_{EFdA\text{-}MP}$

ATP-dependent rescue of $T/P_{EFdA\text{-}MP}$

Template/primer with EFdA-MP at the 3' primer terminus ($T/P_{EFdA\text{-}MP}$) was prepared by incubating 500 nM $T_{d31}/P_{d18\text{-}P0}$ with 1 μM HIV-1 RT in RT buffer and 6 mM $MgCl_2$. EFdA-TP was added into the reaction and the mixture was incubated at 37°C for 1 h. After incorporation of EFdA-TP, the $T/P_{EFdA\text{-}MP}$ was purified using the QIAquick nucleotide removal kit (Qiagen, Valencia, CA). Under these conditions, the extension of T/P to $T/P_{EFdA\text{-}MP}$ was complete. 20 nM of purified $T_{d31}/P_{d18\text{-}P0\text{-}EFdA\text{-}MP}$ was incubated with 60 nM WT or K65R HIV-1 RT in the presence of 3.5 mM ATP, 100 μM dATP, 0.5 μM dTTP, and 10 μM ddGTP in RT buffer and 10 mM $MgCl_2$. Aliquots of the reaction were stopped at different time points (0–90 min). The data from at least four independent experiments were analyzed using GraphPad Prism 4.

PPi-dependent rescue of $T/P_{EFdA\text{-}MP}$

20 nM of purified $T_{d31}/P_{d18\text{-}P0\text{-}EFdA\text{-}MP}$ was incubated at 37°C with 60 nM WT or K65R HIV-1 RT in the presence of 150 μM PPi, 100 μM dATP, 0.5 μM dTTP, and 10 μM ddGTP in RT buffer and 6 mM $MgCl_2$. Aliquots of the reaction were stopped at different times (0–40 min). The data from at least two independent experiments were plotted using GraphPad Prism 4.

Molecular modeling

Molecular models of dATP and EFdA-TP in the active site of WT HIV RT were made using PDB ID 1 T05 [72] as a starting model (WT HIV RT in complex with tenofovir diphosphate). A molecular model of EFdA-TP in the active site of K65R HIV RT was made using PDB ID 3JYT [44] as a starting model (K65R HIV RT in complex with dATP). The sketch module of SYBYL (Version 7.3.5, Tripos International, St. Louis, MO) was used to make dATP and EFdA-TP molecules. dATP and EFdA-TP were each superposed to tenofovir diphosphate in the WT complex, after which the tenofovir diphosphate was removed. Gasteiger-Huckel charges were calculated and molecular minimization of the WT-dATP and WT-EFdA-TP were performed in SYBYL using the Powell method. SYBYL was also used to add the 2-fluoro and 4'-ethynyl groups to dATP in the K65R complex. Gasteiger-Huckel charges were then calculated and molecular minimization was performed as for the WT complexes.

Additional file

Additional file 1: Figure S1. Effect of K65R mutation on the formation of RT:T/$P_{EFdA\text{-}MP}$ complex. Purified T/$P_{EFdA\text{-}MP}$ (25 nM) was incubated at room temperature for 10 min with different concentrations of WT or K65R RTs in RT buffer and 6 mM $MgCl_2$. RT was used at different concentrations to obtain RT:DNA ratios that ranged from 0 to 10. Four μl of 20% sucrose was added to each mixture in a final volume of 24 μl. The complexes were subsequently resolved on a native 6% polyacrylamide Tris borate gel and visualized as described in Methods.

Abbreviations

HIV: Human immunodeficiency virus; RT: Reverse transcriptase; NRTI: Nucleoside reverse transcriptase inhibitor; TDRTI: Translocation-defective RT inhibitor; EFdA: 4'-ethynyl-2-fluoro-2'-deoxyadenosine; MP: Monophosphate; TP: Triphosphate; TDF: Tenofovir disoproxil fumarate; T/P: Template/primer; T/$P_{EFdA\text{-}MP}$: Template/primer possessing EFdA-MP at the 3'-primer terminus (or T/P chain terminated by EFdA-MP).

Competing interests

Hiroaki Mitsuya and Eiichi Kodama are inventors of EFdA.

Authors' contributions

EM designed the biochemical experiments. EM and EMR carried out the biochemical experiments. MDL, ADH, and KS assisted in some of the biochemical experiments. AH designed and carried out the cell-based assays. KAK and SGS performed the molecular modeling studies. YTO and JCJ participated in the initial biochemical studies. BM participated in the design of biochemical experiments and interpretation of data. ENK, HM, and MAP helped with preliminary virological data. MAP helped in the data interpretation. EM drafted the manuscript. SGS conceived and coordinated the study and drafted the manuscript. All authors read and approved the final manuscript.

Acknowledgements

Dr. Tatiana Ilina's contribution in the preparation of the RT plasmids is acknowledged. This work was supported, in whole or in part, by National Institutes of Health grants AI076119, AI074389, AI076119-S1, AI076119-02S1, AI100890, AI099284, and GM103368 (S. G. S.) and AI079801 (M. A. P.).

Author details

[1]Christopher Bond Life Sciences Center, Department of Molecular Microbiology & Immunology, University of Missouri, Columbia, MO 65211, USA. [2]Clinical Research Center, Department of Infectious Diseases and Immunology, National Hospital Organization Nagoya Medical Center, Nagoya 4600001, Japan. [3]Division of Emerging Infectious Diseases, Tohoku University, Sendai 980-8575, Japan. [4]Department of Internal Medicine, Kumamoto University, Kumamoto 860-8556, Japan. [5]Experimental Retrovirology Section, HIV/AIDS Malignancy Branch, NIH, Bethesda, MD 20892, USA. [6]Department of Microbiology and Molecular Genetics, University of Pittsburgh, Pittsburgh, PA 15219, USA. [7]Department of Biochemistry, University of Missouri, Columbia, MO 65211, USA.

Received: 22 April 2013 Accepted: 13 June 2013
Published: 24 June 2013

References

1. Parniak MA, Sluis-Cremer N: **Inhibitors of HIV-1 reverse transcriptase.** *Advances in pharmacology (San Diego, Calif)* 2000, **49**:67–109.
2. Sharma PL, Nurpeisov V, Hernandez-Santiago B, Beltran T, Schinazi RF: **Nucleoside inhibitors of human immunodeficiency virus type 1 reverse transcriptase.** *Curr Top Med Chem* 2004, **4**:895–919.
3. Hammer SM, Saag MS, Schechter M, Montaner JS, Schooley RT, Jacobsen DM, Thompson MA, Carpenter CC, Fischl MA, Gazzard BG, *et al*: **Treatment for adult HIV infection: 2006 recommendations of the International AIDS Society–USA panel.** *Top HIV Med* 2006, **14**:827–843.
4. Schinazi RF, Hernandez-Santiago BI, Hurwitz SJ: **Pharmacology of current and promising nucleosides for the treatment of human immunodeficiency viruses.** *Antiviral Res* 2006, **71**:322–334.
5. De Clercq E: **Anti-HIV drugs.** *Verh K Acad Geneeskd Belg* 2007, **69**:81–104.
6. Sluis-Cremer N, Tachedjian G: **Mechanisms of inhibition of HIV replication by non-nucleoside reverse transcriptase inhibitors.** *Virus Res* 2008, **134**:147–156.
7. Deval J: **Antimicrobial strategies: inhibition of viral polymerases by 3'-hydroxyl nucleosides.** *Drugs* 2009, **69**:151–166.
8. Sarafianos SG, Marchand B, Das K, Himmel DM, Parniak MA, Hughes SH, Arnold E: **Structure and Function of HIV-1 Reverse Transcriptase: Molecular Mechanisms of Polymerization and Inhibition.** *J Mol Biol* 2009, **385**:693–713.
9. Ren J, Esnouf R, Garman E, Somers D, Ross C, Kirby I, Keeling J, Darby G, Jones Y, Stuart D, *et al*: **High resolution structures of HIV-1 RT from four RT-inhibitor complexes.** *Nat Struct Biol* 1995, **2**:293–302.
10. Ding J, Das K, Hsiou Y, Sarafianos SG, Clark AD Jr, Jacobo-Molina A, Tantillo C, Hughes SH, Arnold E: **Structure and functional implications of the polymerase active site region in a complex of HIV-1 RT with a double-stranded DNA template-primer and an antibody Fab fragment at 2.8 A resolution.** *J Mol Biol* 1998, **284**:1095–1111.
11. Kohlstaedt LA, Wang J, Friedman JM, Rice PA, Steitz TA: **Crystal structure at 3.5 A resolution of HIV-1 reverse transcriptase complexed with an inhibitor.** *Science* 1992, **256**:1783–1790.
12. Rodgers DW, Gamblin SJ, Harris BA, Ray S, Culp JS, Hellmig B, Woolf DJ, Debouck C, Harrison SC: **The structure of unliganded reverse transcriptase from the human immunodeficiency virus type 1.** *Proc Natl Acad Sci USA* 1995, **92**:1222–1226.
13. Hsiou Y, Ding J, Das K, Clark AD Jr, Hughes SH, Arnold E: **Structure of unliganded HIV-1 reverse transcriptase at 2.7 A resolution: implications of conformational changes for polymerization and inhibition mechanisms.** *Structure* 1996, **4**:853–860.
14. Spence RA, Kati WM, Anderson KS, Johnson KA: **Mechanism of inhibition of HIV-1 reverse transcriptase by nonnucleoside inhibitors.** *Science* 1995, **267**:988–993.
15. Rittinger K, Divita G, Goody RS: **Human immunodeficiency virus reverse transcriptase substrate-induced conformational changes and the mechanism of inhibition by nonnucleoside inhibitors.** *Proc Natl Acad Sci USA* 1995, **92**:8046–8049.
16. Sluis-Cremer N, Arion D, Parniak MA: **Molecular mechanisms of HIV-1 resistance to nucleoside reverse transcriptase inhibitors (NRTIs).** *Cell Mol Life Sci* 2000, **57**:1408–1422.
17. Menendez-Arias L: **Mechanisms of resistance to nucleoside analogue inhibitors of HIV-1 reverse transcriptase.** *Virus Res* 2008, **134**:124–146.
18. Martin-Hernandez AM, Domingo E, Menendez-Arias L: **Human immunodeficiency virus type 1 reverse transcriptase: role of Tyr115 in deoxynucleotide binding and misinsertion fidelity of DNA synthesis.** *EMBO J* 1996, **15**:4434–4442.
19. Gao G, Orlova M, Georgiadis MM, Hendrickson WA, Goff SP: **Conferring RNA polymerase activity to a DNA polymerase: a single residue in reverse transcriptase controls substrate selection.** *Proc Natl Acad Sci USA* 1997, **94**:407–411.
20. Gao HQ, Boyer PL, Sarafianos SG, Arnold E, Hughes SH: **The role of steric hindrance in 3TC resistance of human immunodeficiency virus type-1 reverse transcriptase.** *J Mol Biol* 2000, **300**:403–418.
21. Sarafianos SG, Das K, Clark AD Jr, Ding J, Boyer PL, Hughes SH, Arnold E: **Lamivudine (3TC) resistance in HIV-1 reverse transcriptase involves steric hindrance with beta-branched amino acids.** *Proc Natl Acad Sci USA* 1999, **96**:10027–10032.
22. Tisdale M, Kemp SD, Parry NR, Larder BA: **Rapid in vitro selection of human immunodeficiency virus type 1 resistant to 3'-thiacytidine inhibitors due to a mutation in the YMDD region of reverse transcriptase.** *Proc Natl Acad Sci USA* 1993, **90**:5653–5656.
23. Feng JY, Anderson KS: **Mechanistic studies examining the efficiency and fidelity of DNA synthesis by the 3TC-resistant mutant (184V) of HIV-1 reverse transcriptase.** *Biochemistry* 1999, **38**:9440–9448.
24. Back NK, Nijhuis M, Keulen W, Boucher CA, Oude Essink BO, van Kuilenburg AB, van Gennip AH, Berkhout B: **Reduced replication of 3TC-resistant HIV-1 variants in primary cells due to a processivity defect of the reverse transcriptase enzyme.** *EMBO J* 1996, **15**:4040–4049.
25. Arion D, Kaushik N, McCormick S, Borkow G, Parniak MA: **Phenotypic mechanism of HIV-1 resistance to 3'-azido-3'-deoxythymidine (AZT): increased polymerization processivity and enhanced sensitivity to pyrophosphate of the mutant viral reverse transcriptase.** *Biochemistry* 1998, **37**:15908–15917.
26. Meyer PR, Matsuura SE, So AG, Scott WA: **Unblocking of chain-terminated primer by HIV-1 reverse transcriptase through a nucleotide-dependent mechanism.** *Proc Natl Acad Sci USA* 1998, **95**:13471–13476.

27. Meyer PR, Matsuura SE, Mian AM, So AG, Scott WA: **A mechanism of AZT resistance: an increase in nucleotide-dependent primer unblocking by mutant HIV-1 reverse transcriptase.** *Mol Cell* 1999, **4**:35–43.
28. Meyer PR, Matsuura SE, Tolun AA, Pfeifer I, So AG, Mellors JW, Scott WA: **Effects of specific zidovudine resistance mutations and substrate structure on nucleotide-dependent primer unblocking by human immunodeficiency virus type 1 reverse transcriptase.** *Antimicrob Agents Chemother* 2002, **46**:1540–1545.
29. Boyer PL, Sarafianos SG, Arnold E, Hughes SH: **Selective excision of AZTMP by drug-resistant human immunodeficiency virus reverse transcriptase.** *J Virol* 2001, **75**:4832–4842.
30. Larder BA, Kemp SD: **Multiple mutations in HIV-1 reverse transcriptase confer high-level resistance to zidovudine (AZT).** *Science* 1989, **246**:1155–1158.
31. Winters MA, Shafer RW, Jellinger RA, Mamtora G, Gingeras T, Merigan TC: **Human immunodeficiency virus type 1 reverse transcriptase genotype and drug susceptibility changes in infected individuals receiving dideoxyinosine monotherapy for 1 to 2 years.** *Antimicrob Agents Chemother* 1997, **41**:757–762.
32. Harrigan PR, Stone C, Griffin P, Najera I, Bloor S, Kemp S, Tisdale M, Larder B: **Resistance profile of the human immunodeficiency virus type 1 reverse transcriptase inhibitor abacavir (1592U89) after monotherapy and combination therapy. CNA2001 Investigative Group.** *J Infect Dis* 2000, **181**:912–920.
33. Margot NA, Lu B, Cheng A, Miller MD, Study T: **Resistance development over 144 weeks in treatment-naive patients receiving tenofovir disoproxil fumarate or stavudine with lamivudine and efavirenz in Study 903.** *HIV Med* 2006, **7**:442–450.
34. Wainberg MA, Miller MD, Quan Y, Salomon H, Mulato AS, Lamy PD, Margot NA, Anton KE, Cherrington JM: **In vitro selection and characterization of HIV-1 with reduced susceptibility to PMPA.** *Antivir Ther* 1999, **4**:87–94.
35. Margot NA, Isaacson E, McGowan I, Cheng AK, Schooley RT, Miller MD: **Genotypic and phenotypic analyses of HIV-1 in antiretroviral-experienced patients treated with tenofovir DF.** *AIDS* 2002, **16**:1227–1235.
36. Feng JY, Myrick FT, Margot NA, Mulamba GB, Rimsky L, Borroto-Esoda K, Selmi B, Canard B: **Virologic and enzymatic studies revealing the mechanism of K65R- and Q151M-associated HIV-1 drug resistance towards emtricitabine and lamivudine.** *Nucleosides Nucleotides Nucleic Acids* 2006, **25**:89–107.
37. Shah FS, Curr KA, Hamburgh ME, Parniak M, Mitsuya H, Arnez JG, Prasad VR: **Differential influence of nucleoside analog-resistance mutations K65R and L74V on the overall mutation rate and error specificity of human immunodeficiency virus type 1 reverse transcriptase.** *J Biol Chem* 2000, **275**:27037–27044.
38. Frankel FA, Invernizzi CF, Oliveira M, Wainberg MA: **Diminished efficiency of HIV-1 reverse transcriptase containing the K65R and M184V drug resistance mutations.** *AIDS* 2007, **21**:665–675.
39. Parikh UM, Zelina S, Sluis-Cremer N, Mellors JW: **Molecular mechanisms of bidirectional antagonism between K65R and thymidine analog mutations in HIV-1 reverse transcriptase.** *AIDS* 2007, **21**:1405–1414.
40. White KL, Margot NA, Ly JK, Chen JM, Ray AS, Pavelko M, Wang R, McDermott M, Swaminathan S, Miller MD: **A combination of decreased NRTI incorporation and decreased excision determines the resistance profile of HIV-1 K65R RT.** *AIDS* 2005, **19**:1751–1760.
41. Deval J, Navarro JM, Selmi B, Courcambeck J, Boretto J, Halfon P, Garrido-Urbani S, Sire J, Canard B: **A loss of viral replicative capacity correlates with altered DNA polymerization kinetics by the human immunodeficiency virus reverse transcriptase bearing the K65R and L74V dideoxynucleoside resistance substitutions.** *J Biol Chem* 2004, **279**:25489–25496.
42. Deval J, White KL, Miller MD, Parkin NT, Courcambeck J, Halfon P, Selmi B, Boretto J, Canard B: **Mechanistic basis for reduced viral and enzymatic fitness of HIV-1 reverse transcriptase containing both K65R and M184V mutations.** *J Biol Chem* 2004, **279**:509–516.
43. White KL, Chen JM, Feng JY, Margot NA, Ly JK, Ray AS, Macarthur HL, McDermott MJ, Swaminathan S, Miller MD: **The K65R reverse transcriptase mutation in HIV-1 reverses the excision phenotype of zidovudine resistance mutations.** *Antivir Ther* 2006, **11**:155–163.
44. Das K, Bandwar RP, White KL, Feng JY, Sarafianos SG, Tuske S, Tu X, Clark AD Jr, Boyer PL, Hou X, *et al:* **Structural basis for the role of the K65R mutation in HIV-1 reverse transcriptase polymerization, excision antagonism, and tenofovir resistance.** *J Biol Chem* 2009, **284**:35092–35100.
45. Kawamoto A, Kodama E, Sarafianos SG, Sakagami Y, Kohgo S, Kitano K, Ashida N, Iwai Y, Hayakawa H, Nakata H, *et al:* **2'-deoxy-4'-C-ethynyl-2-halo-adenosines active against drug-resistant human immunodeficiency virus type 1 variants.** *Int J Biochem Cell Biol* 2008, **40**:2410–2420.
46. Michailidis E, Marchand B, Kodama EN, Singh K, Matsuoka M, Kirby KA, Ryan EM, Sawani AM, Nagy E, Ashida N, *et al:* **Mechanism of inhibition of HIV-1 reverse transcriptase by 4'-Ethynyl-2-fluoro-2'-deoxyadenosine triphosphate, a translocation-defective reverse transcriptase inhibitor.** *J Biol Chem* 2009, **284**:35681–35691.
47. Marchand B, Gotte M: **Site-specific footprinting reveals differences in the translocation status of HIV-1 reverse transcriptase. Implications for polymerase translocation and drug resistance.** *J Biol Chem* 2003, **278**:35362–35372.
48. Ray AS, Murakami E, Basavapathruni A, Vaccaro JA, Ulrich D, Chu CK, Schinazi RF, Anderson KS: **Probing the molecular mechanisms of AZT drug resistance mediated by HIV-1 reverse transcriptase using a transient kinetic analysis.** *Biochemistry* 2003, **42**:8831–8841.
49. Tu X, Das K, Han Q, Bauman JD, Clark AD Jr, Hou X, Frenkel YV, Gaffney BL, Jones RA, Boyer PL, *et al:* **Structural basis of HIV-1 resistance to AZT by excision.** *Nat Struct Mol Biol* 2010, **17**:1202–1209.
50. Winters B, Montaner J, Harrigan PR, Gazzard B, Pozniak A, Miller MD, Emery S, van Leth F, Robinson P, Baxter JD, *et al:* **Determination of clinically relevant cutoffs for HIV-1 phenotypic resistance estimates through a combined analysis of clinical trial and cohort data.** *J Acquir Immune Defic Syndr* 2008, **48**:26–34.
51. Murphey-Corb M, Rajakumar P, Michael H, Nyaundi J, Didier PJ, Reeve AB, Mitsuya H, Sarafianos SG, Parniak MA: **Response of simian immunodeficiency virus to the novel nucleoside reverse transcriptase inhibitor 4'-ethynyl-2-fluoro-2'-deoxyadenosine in vitro and in vivo.** *Antimicrob Agents Chemother* 2012, **56**:4707–4712.
52. St Clair MH, Martin JL, Tudor-Williams G, Bach MC, Vavro CL, King DM, Kellam P, Kemp SD, Larder BA: **Resistance to ddI and sensitivity to AZT induced by a mutation in HIV-1 reverse transcriptase.** *Science* 1991, **253**:1557–1559.
53. Quan Y, Gu Z, Li X, Liang C, Parniak MA, Wainberg MA: **Endogenous reverse transcriptase assays reveal synergy between combinations of the M184V and other drug resistance-conferring mutations in interactions with nucleoside analog triphosphates.** *J Mol Biol* 1998, **277**:237–247.
54. Bazmi HZ, Hammond JL, Cavalcanti SC, Chu CK, Schinazi RF, Mellors JW: **In vitro selection of mutations in the human immunodeficiency virus type 1 reverse transcriptase that decrease susceptibility to (–)-beta-D-dioxolane-guanosine and suppress resistance to 3'-azido-3'-deoxythymidine.** *Antimicrob Agents Chemother* 2000, **44**:1783–1788.
55. Parikh UM, Bacheler L, Koontz D, Mellors JW: **The K65R mutation in human immunodeficiency virus type 1 reverse transcriptase exhibits bidirectional phenotypic antagonism with thymidine analog mutations.** *J Virol* 2006, **80**:4971–4977.
56. Kodama EI, Kohgo S, Kitano K, Machida H, Gatanaga H, Shigeta S, Matsuoka M, Ohrui H, Mitsuya H: **4'-Ethynyl nucleoside analogs: potent inhibitors of multidrug-resistant human immunodeficiency virus variants in vitro.** *Antimicrob Agents Chemother* 2001, **45**:1539–1546.
57. Larder BA: **3'-Azido-3'-deoxythymidine resistance suppressed by a mutation conferring human immunodeficiency virus type 1 resistance to nonnucleoside reverse transcriptase inhibitors.** *Antimicrob Agents Chemother* 1992, **36**:2664–2669.
58. Selmi B, Deval J, Alvarez K, Boretto J, Sarfati S, Guerreiro C, Canard B: **The Y181C substitution in 3'-azido-3'-deoxythymidine-resistant human immunodeficiency virus, type 1, reverse transcriptase suppresses the ATP-mediated repair of the 3'-azido-3'-deoxythymidine 5'-monophosphate-terminated primer.** *J Biol Chem* 2003, **278**:40464–40472.
59. Boucher CA, Cammack N, Schipper P, Schuurman R, Rouse P, Wainberg MA, Cameron JM: **High-level resistance to (–) enantiomeric 2'-deoxy-3'-thiacytidine in vitro is due to one amino acid substitution in the catalytic site of human immunodeficiency virus type 1 reverse transcriptase.** *Antimicrob Agents Chemother* 1993, **37**:2231–2234.
60. Boyer PL, Sarafianos SG, Arnold E, Hughes SH: **The M184V mutation reduces the selective excision of zidovudine 5'-monophosphate (AZTMP) by the reverse transcriptase of human immunodeficiency virus type 1.** *J Virol* 2002, **76**:3248–3256.
61. Gotte M, Arion D, Parniak MA, Wainberg MA: **The M184V mutation in the reverse transcriptase of human immunodeficiency virus type 1 impairs rescue of chain-terminated DNA synthesis.** *J Virol* 2000, **74**:3579–3585.

62. Hachiya A, Marchand B, Kirby KA, Michailidis E, Tu X, Palczewski K, Ong YT, Li Z, Griffin DT, Schuckmann MM, *et al:* **HIV-1 reverse transcriptase (RT) polymorphism 172K suppresses the effect of clinically relevant drug resistance mutations to both nucleoside and non-nucleoside RT inhibitors.** *J Biol Chem* 2012, **287:**29988–29999.
63. Hachiya A, Gatanaga H, Kodama E, Ikeuchi M, Matsuoka M, Harada S, Mitsuya H, Kimura S, Oka S: **Novel patterns of nevirapine resistance-associated mutations of human immunodeficiency virus type 1 in treatment-naive patients.** *Virology* 2004, **327:**215–224.
64. Hachiya A, Kodama EN, Sarafianos SG, Schuckmann MM, Sakagami Y, Matsuoka M, Takiguchi M, Gatanaga H, Oka S: **Amino acid mutation N348I in the connection subdomain of human immunodeficiency virus type 1 reverse transcriptase confers multiclass resistance to nucleoside and nonnucleoside reverse transcriptase inhibitors.** *J Virol* 2008, **82:**3261–3270.
65. Bauman JD, Das K, Ho WC, Baweja M, Himmel DM, Clark AD Jr, Oren DA, Boyer PL, Hughes SH, Shatkin AJ, Arnold E: **Crystal engineering of HIV-1 reverse transcriptase for structure-based drug design.** *Nucleic Acids Res* 2008, **36:**5083–5092.
66. Schuckmann MM, Marchand B, Hachiya A, Kodama EN, Kirby KA, Singh K, Sarafianos SG: **The N348I mutation at the connection subdomain of HIV-1 reverse transcriptase decreases binding to nevirapine.** *J Biol Chem* 2010, **285:**38700–38709.
67. Ndongwe TP, Adedeji AO, Michailidis E, Ong YT, Hachiya A, Marchand B, Ryan EM, Rai DK, Kirby KA, Whatley AS, *et al:* **Biochemical, inhibition and inhibitor resistance studies of xenotropic murine leukemia virus-related virus reverse transcriptase.** *Nucleic Acids Res* 2012, **40:**345–359.
68. Kirby KA, Marchand B, Ong YT, Ndongwe TP, Hachiya A, Michailidis E, Leslie MD, Sietsema DV, Fetterly TL, Dorst CA, *et al:* **Structural and Inhibition Studies of the RNase H Function of Xenotropic Murine Leukemia Virus-Related Virus Reverse Transcriptase.** *Antimicrob Agents Chemother* 2012, **56**(4):2048–61.
69. Sarafianos SG, Clark AD Jr, Tuske S, Squire CJ, Das K, Sheng D, Ilankumaran P, Ramesha AR, Kroth H, Sayer JM, *et al:* **Trapping HIV-1 reverse transcriptase before and after translocation on DNA.** *J Biol Chem* 2003, **278:**16280–16288.
70. Ohrui H, Kohgo S, Hayakawa H, Kodama E, Matsuoka M, Nakata T, Mitsuya H: **2'-deoxy-4'-C-ethynyl-2-fluoroadenosine: a nucleoside reverse transcriptase inhibitor with highly potent activity against wide spectrum of HIV-1 strains, favorable toxic profiles, and stability in plasma.** *Nucleosides Nucleotides Nucleic Acids* 2007, **26**(10-12):1543–6.
71. Biaglow JE, Kachur AV: **The generation of hydroxyl radicals in the reaction of molecular oxygen with polyphosphate complexes of ferrous ion.** *Radiat Res* 1997, **148:**181–187.
72. Tuske S, Sarafianos SG, Clark AD Jr, Ding J, Naeger LK, White KL, Miller MD, Gibbs CS, Boyer PL, Clark P, *et al:* **Structures of HIV-1 RT-DNA complexes before and after incorporation of the anti-AIDS drug tenofovir.** *Nat Struct Mol Biol* 2004, **11:**469–474.

doi:10.1186/1742-4690-10-65
Cite this article as: Michailidis *et al.*: Hypersusceptibility mechanism of Tenofovir-resistant HIV to EFdA. *Retrovirology* 2013 **10**:65.

AAC
Journals.ASM.org

Evaluation of Combinations of 4′-Ethynyl-2-Fluoro-2′-Deoxyadenosine with Clinically Used Antiretroviral Drugs

Atsuko Hachiya,[a,b]* Aaron B. Reeve,[c] Bruno Marchand,[a] Eleftherios Michailidis,[a] Yee Tsuey Ong,[a] Karen A. Kirby,[a] Maxwell D. Leslie,[a] Shinichi Oka,[b] Eiichi N. Kodama,[d] Lisa C. Rohan,[e,f] Hiroaki Mitsuya,[g,h] Michael A. Parniak,[c] Stefan G. Sarafianos[a,i]

Christopher Bond Life Sciences Center, Department of Molecular Microbiology and Immunology, University of Missouri School of Medicine, Columbia, Missouri, USA[a]; AIDS Clinical Center, National Center for Global Health and Medicine, Tokyo, Japan[b]; Department of Microbiology and Molecular Genetics, University of Pittsburgh, Pittsburgh, Pennsylvania, USA[c]; Division of Emerging Infectious Diseases, Tohoku University, Tohoku Medical Megabank Organization, Miyagi, Japan[d]; Magee-Womens Research Institute[e] and Department of Pharmaceutical Sciences, School of Pharmacy,[f] University of Pittsburgh, Pittsburgh, Pennsylvania, USA; Department of Hematology and Infectious Diseases, Kumamoto University, Kumamoto, Japan[g]; Experimental Retrovirology Section, HIV/AIDS Malignancy Branch, National Institutes of Health, Bethesda, Maryland, USA[h]; Department of Biochemistry, University of Missouri, Columbia, Missouri, USA[i]

Drug combination studies of 4′-ethynyl-2-fluoro-2′-deoxyadenosine (EFdA) with FDA-approved drugs were evaluated by two different methods, MacSynergy II and CalcuSyn. Most of the combinations, including the combination of the two adenosine analogs EFdA and tenofovir, were essentially additive, without substantial antagonism or synergism. The combination of EFdA and rilpivirine showed apparent synergism. These studies provide information that may be useful for the design of EFdA combination regimens for initial and salvage therapy assessment.

Combination antiretroviral therapies provide durable viral suppression and constitute the standard of care for HIV infection (http://www.aidsinfo.nih.gov/guidelines/) (1). For example, the combination of tenofovir disoproxil fumarate (TDF) and emtricitabine (FTC) (Truvada) is one of the preferred regimens for treatment of HIV-1 infection (2, 3). *In vitro* studies have shown that tenofovir (TFV) and FTC have synergistic antiretroviral activity (4, 5).

The investigational nucleoside reverse transcriptase inhibitor (NRTI), 4′-ethynyl-2-fluoro-2′-deoxyadenosine (EFdA) is presently under preclinical evaluation. Unlike other NRTIs used in the treatment of HIV infection, EFdA retains the 3′-hydroxyl moiety. It also contains a 2-fluoro group on the adenine base and a 4′-ethynyl group on the deoxyribose ring. Although EFdA is an adenosine analog, its activation is initiated by phosphorylation by 2′-deoxycytidine kinase (dCK), and the drug is highly resistant to degradation by adenosine deaminase (ADA) (6). EFdA shows exceptional antiretroviral activity *in vitro* (6–8) and *in vivo* (9, 10) as well as a favorable cross-resistance profile with current reverse transcriptase inhibitors (RTIs) used in the clinic.

Studies on potential interactions between EFdA and other antiretroviral drugs can provide information that could be useful in the development of combinatorial therapeutic strategies. The present study evaluates anti-HIV efficacy in combinations of EFdA with representative FDA-approved RTIs *in vitro*.

We first determined the antiviral potencies of five NRTIs (zidovudine [AZT], lamivudine [3TC], FTC, TDF, and EFdA) and three nonnucleoside RTIs (NNRTIs; efavirenz [EFV], etravirine [ETR], and rilpivirine [RPV]) against HIV-1_{NL4-3} in order to obtain an optimal range of drug concentrations for use in combination assay analyses. As previously demonstrated (6, 7), EFdA inhibited HIV-1 replication several orders of magnitude more efficiently than other currently approved NRTIs (Table 1). In the same cell-based assays, we evaluated antiretroviral activity of EFdA in combination with the FDA-approved RTIs. To obtain more comprehensive evaluations of drug combinations and to reduce analysis bias, we use two algorithms provided by the software packages MacSynergy II (version 1.0; Ann Arbor, MI) and CalcuSyn (Biosoft, Ferguson, MO), which are based on the Bliss independence model (11, 12) and the median effect principle (13), respectively. Quantitative differences in data analyses by the two algorithms used by the MacSynergy II and CalcuSyn programs are not uncommon (14). In the present work, drug interactions were considered significant only if detected by both computational approaches.

TABLE 1 Antiviral activity of HIV-1 inhibitors

Compound class and name	EC_{50} (nM) for anti-HIV-1 activity[a]
NRTI	
AZT	180 ± 60
3TC	1,210 ± 240
FTC	370 ± 70
TDF	14 ± 2
EFdA	3 ± 1
NNRTI	
EFV	1.6 ± 0.4
ETR	1 ± 0.1
RPV	0.4 ± 0.1

[a] EC_{50}, 50% effective concentration. Values were determined using the TZM-bl cell line obtained from the NIH AIDS Research and Reference Reagent Program. All assays were conducted in triplicates. The data shown are mean values ± standard deviations obtained from the results of at least three independent experiments.

Received 25 February 2013 **Returned for modification** 6 April 2013
Accepted 15 June 2013
Published ahead of print 24 June 2013
Address correspondence to Stefan G. Sarafianos, sarafianoss@missouri.edu.
* Present address: Atsuko Hachiya, Clinical Research Center, Department of Infectious Diseases and Immunology, National Hospital Organization Nagoya Medical Center, Nagoya, Japan.
A.H. and A.B.R. contributed equally to this article.

doi:10.1128/AAC.00283-13

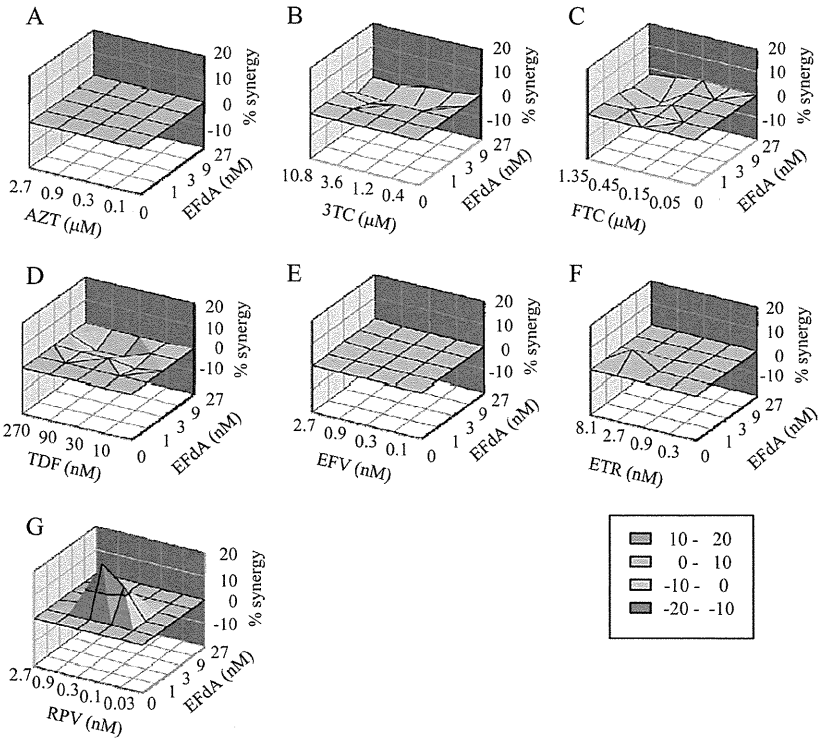

FIG 1 Effects of EFdA in combination with other anti-HIV-1 agents. The calculated additive surface, which represents the predicted additive interactions, is then subtracted from the experimental surface to reveal regions of greater-than-expected interactions (synergy). A resulting surface appearing as a horizontal plane at 0% inhibition above the calculated additive surface suggests that the interactions are merely additive. Peaks of statistically significant synergy (positive value) or antagonism (negative value) that deviate significantly from the expected additive drug interactions derived from 95% confidence interval data are shown in the different plots of the interaction between EFdA and other anti-HIV-1 agents in the cell-based assay, as follows: AZT (A), 3TC (B), FTC (C), TDF (D), EFV (E), ETR (F), and RPV (G). Units of $\mu M^2\%$ are analogous to the units for area under a dose-response curve in the two-dimensional situation.

Most drugs tested, including the adenosine analog TDF, showed little or no drug interactions in combination with EFdA (Fig. 1 and Table 2). Data analysis with CalcuSyn suggested that the combinations of both EFdA and 3TC (EFdA-3TC) and EFdA-FTC are moderately antagonistic (Fig. 1 and Table 2). Using MacSynergy, the EFdA-3TC combination was assessed as minor antagonism, whereas the EFdA-FTC combination was considered additive; however, its value ($-23.4\ \mu M^2\%$) was very close to minor antagonism ($-25\ \mu M^2\%$). The observed borderline antagonism may arise from competition at the first and rate-limiting

TABLE 2 Interactions of drug combinations for inhibition of HIV-1 virus or RT enzyme

Drug class and EFdA combination	Target	MacSynergy analysis		CalcuSyn analysis		
		Synergy/antagonism ($\mu M^2\%$)[a]	Predicted interaction	CI[b]	Predicted interaction	Proposed interaction[c]
NRTI						
AZT	Virus	0/0	Additive	1.18	Additive	Neutral
TDF	Virus	0/−12.8	Additive	1.36	Moderate antagonism	Neutral
3TC	Virus	0/−39.5	Minor antagonism	1.23	Moderate antagonism	Possible antagonism
FTC	Virus	0/−23.4	Additive	1.25	Moderate antagonism	Neutral
NNRTI						
EFV	Virus	1.9/0	Additive	0.9	Additive	Neutral
ETR	Virus	7.8/0	Additive	1.05	Additive	Neutral
RPV	Virus	41.0/−0.04	Minor synergy	0.64	Synergy	Synergy
RPV	Enzyme	34.1/0	Minor synergy	0.56	Synergy	Synergy

[a] The volume of the peaks in the difference plots at the 95% confidence level, which corresponds to the area under a dose-response curve and is considered to provide a quantitative measure of possible drug interactions. MacSynergy II defines $\mu M^2\%$ values as follows: 25 to 50, minor synergy; 50 to 100, moderate synergy; >100, strong synergy. The corresponding negative value ranges reflect minor, moderate, and strong antagonism, respectively. Values between 25 and $-25\ \mu M^2\%$ are considered insignificant.

[b] CI, combination Index. CalcuSyn defines CI values as follows: 0.1 to 0.3, strong synergy; 0.3 to 0.7, synergy; 0.7 to 0.85, moderate synergy; 0.85 to 1.2, additive; 1.2 to 1.45, moderate antagonism; 1.45 to 3.3, antagonism; 3.3 to 10, strong antagonism.

[c] Proposed interaction is assessed on the basis of the predictions by the two computational methods. Neutral, a lack of drug interaction in the combination (additivity).

TABLE 3 Antiviral and prophylactic activity of EFdA, RPV, and EFdA-RPV combinations

Activity type (pretreatment) and virus	Drug treatment[a]	EC_{50} (nM)[b]	CI_{50}[c]
Antiviral activity			
Wild type	EFdA	0.9 ± 0.2	
	RPV	0.7 ± 0.1	
	EFdA-RPV	0.4 ± 0.2	0.55
M184V	EFdA	15 ± 3	
	RPV	0.6 ± 0.2	
	EFdA-RPV	0.7 ± 0.1	0.5
L100I/K103N	EFdA	1 ± 0.5	
	RPV	10 ± 2	
	EFdA-RPV	9 ± 2	0.45
Prophylaxis (2-h preincubation)			
Wild type	EFdA	11 ± 5	
	RPV	18 ± 4	
	EFdA-RPV	5 ± 2	0.75
M184V	EFdA	97 ± 22	
	RPV	8 ± 2	
	EFdA-RPV	10 ± 3	1
L100I/K103N	EFdA	12 ± 3	
	RPV	175 ± 42	
	EFdA-RPV	9 ± 2	0.6
Prophylaxis (18-h preincubation)			
Wild type	EFdA	3 ± 1	
	RPV	21 ± 4	
	EFdA-RPV	4 ± 1	0.9
M184V	EFdA	53 ± 13	
	RPV	14 ± 4	
	EFdA-RPV	13 ± 40	0.6
L100I/K103N	EFdA	6 ± 1	
	RPV	250 ± 25	
	EFdA-RPV	5 ± 2	0.75

[a] EFdA and RPV were combined at a 1:1 ratio.

[b] EC_{50}, 50% effective concentration. The data shown are mean values ± standard deviations obtained from the results of at least three independent experiments using P4R5-MAGI cells (32).

[c] CI_{50} is the calculated combination index at a 50% inhibitory concentration.

phosphorylation step as EFdA, 3TC, and FTC are all initially activated by 2′-deoxycytidine kinase (6, 15, 16). Small differences in the effect of 3TC versus FTC may arise from the longer half-life of FTC. In contrast, the combination of EFdA-RPV demonstrated apparently significant synergy, as assessed by the two different methods (41 μM^2% in MacSynergy and 0.64 combination index [CI] in CalcuSyn). To confirm the synergy of HIV-1 inhibition by EFdA-RPV, we further evaluated this combination in the enzymatic assay for reverse transcriptase. Primer extension assays (7, 17) were performed with Quant-iT PicoGreen reagent (Invitrogen, Carlsbad, CA) (18). As shown in Table 2, the combination of EFdA with RPV provided synergistic effects on inhibition of reverse transcription.

We further compared the antiretroviral activity of various concentrations of EFdA alone, RPV alone, and a 1:1 molar combination of EFdA and RPV against wild-type virus and two HIV-1 mutants with reverse transcriptase (RT) mutations M184V and L100I/K103N. To evaluate the ability of the drugs to establish a barrier to subsequent infection in the absence of exogenous drug, cells were pretreated with various concentrations of each drug alone or in combination, followed by removal of exogenous drug and inoculation with HIV-1. These conditions assess intracellular persistence of drug following exogenous drug clearance, which is dependent on the intracellular half-life of the test drugs. The EFdA-RPV combination provided additive to synergistic inhibition of wild-type HIV-1 and both mutant strains (Table 3). The protective effect established by EFdA pretreatment is likely the result of EFdA resistance to degradation by adenosine deaminase (ADA) (6), consistent with a longer intracellular half-life (19). Hence, our data suggest that EFdA could be a strong candidate for use in preexposure prophylaxis, an approach in which TDF has shown efficacy in clinical studies (20, 21).

Finally, we evaluated the ability of EFdA-RPV pretreatment to protect MT-2 lymphoblastoid cells from infection by a mixed virus population consisting of six HIV-1 strains: the wild type; the mutants K65R, Y181C, M184V, and D67N/K70R/T215F/K219Q (thymidine analogue mutations [TAMs]); and L100I/K103N. Cells were exposed to appropriate drugs for 16 h, and then exogenous drug was removed (Fig. 2). The breakthrough virus population harvested from cells not exposed to drug contained all six input viruses, plus some recombinant strains (Fig. 2B). Rapid virus breakthrough was evident in cells pretreated with RPV alone, and the only virus detected in the RPV-breakthrough population was the NNRTI-resistant L100I/K103N (100%). In contrast, breakthrough in cells pretreated with EFdA alone was significantly delayed. The EFdA-breakthrough population contained a mixture of the NRTI-resistant M184V mutant (54%) and TAMs (32%), plus some recombinant strains consisting of M184V plus one or more TAMs. No breakthrough was noted in cells pretreated with the EFdA-RPV combination, suggesting an enhanced protective effect of the drug combination compared to either drug alone.

Synergistic interactions between NRTIs and NNRTIs have been previously reported in both viral (5, 22–24) and enzymatic assays (5, 25–31). NNRTIs may act synergistically with NRTIs by

A

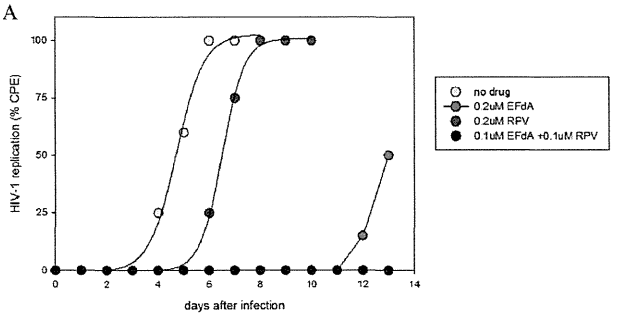

B

Virus	% of breakthrough virus			
	No drug	0.2 μM RPV	0.2 μM EFdA	Combination
Wild-type	20	0	0	-
K65R	15	0	0	-
M184V	3.5	0	54	-
TAMs	6	0	32	-
Y181C	17	0	0	-
L100I/K103N	28	100	0	-
Recombinant	10.5	0	14	-

FIG 2 HIV-1 breakthrough in cells pretreated with EFdA, RPV, or a combination of EFdA and RPV. (A) MT-2 cells were incubated with the indicated concentrations of drug for 18 h and then extensively washed to remove exogenous drug. The washed cells were infected with a mixture of six virus strains (the wild type and five drug-resistant variants). Cells were examined daily for HIV-induced cytopathic effects. (B) Genotypic composition of breakthrough virus is shown. At least 20 clones from each breakthrough virus were sequenced. EFdA (0.1 μM) and RPV (0.1 μM) were used in combination. No virus breakthrough was noted in cells pretreated with the EFdA-RPV combination. TAMs (thymidine analog resistance mutations) included the D67N, K70R, T210F, and T219Q RT mutations. Recombinant virus possessed mutations derived from at least two of the input virus strains.

suppressing the phosphorolytic unblocking of NRTI-terminated primers, possibly by stabilizing the primer terminus at a posttranslocation position, where it cannot undergo phosphorolytic removal (5, 26, 27, 29). The mechanism for the apparent synergistic activity of the EFdA-RPV combination is under investigation.

In conclusion, EFdA in combination with RPV may provide a beneficial interaction against replication of drug-sensitive and certain RTI-resistant HIV-1 strains. The results of the present study indicate that EFdA may act as promising component of future antiretroviral therapies.

ACKNOWLEDGMENTS

This work was supported by a grant for the Bilateral International Collaborative R&D Program from the Korean Food and Drug Administration and the Ministry of Knowledge and Economy (S.G.S.), by National Institutes of Health (NIH) research grants AI076119-S1, AI076119-02S1, AI100890, AI099284, AI094715, AI076119, AI074389, and GM103368 to S.G.S. and AI079801 to M.A.P., and by a Grant-in-Aid for the research on HIV/AIDS (H22-AIDS-001) from the Ministry of Health, Labor, and Welfare of Japan (S.O.). B.M. was the recipient of an amfAR Mathilde Krim Fellowship and a Canadian Institutes of Health Research (CIHR) Fellowship. We acknowledge the Yamasa Corporation for providing EFdA for this study.

H.M. and E.N.K. are coinventors of EFdA.

A.H. carried out the cell-based drug combination assays and wrote the manuscript. A.B.R. carried out the viral breakthrough experiments and studies with drug-resistant HIV and wrote portions of the manuscript. B.M., E.M., Y.T.O., K.A.K., and M.D.L. carried out the biochemical assays. S.G.S., M.A.P., S.O., and H.M. contributed to the design of the study, and S.G.S., L.C.R., E.N.K., and M.A.P. edited the manuscript. All authors read this paper and approved the final manuscript.

REFERENCES

1. **Thompson MA, Aberg JA, Hoy JF, Telenti A, Benson C, Cahn P, Eron JJ, Gunthard HF, Hammer SM, Reiss P, Richman DD, Rizzardini G, Thomas DL, Jacobsen DM, Volberding PA.** 2012. Antiretroviral treatment of adult HIV infection: 2012 recommendations of the International Antiviral Society-USA panel. JAMA **308**:387–402.
2. **James JS.** 2004. FDA approves two combination pills, Epzicom and Truvada; comment on commercial race to once-a-day nucleosides. AIDS Treat News **403**:6. http://www.aidsnews.org/2004/08/epzicom-truvada.html.
3. **Killingley B, Pozniak A.** 2007. The first once-daily single-tablet regimen for the treatment of HIV-infected patients. Drugs Today **43**:427–442.
4. **Borroto-Esoda K, Vela JE, Myrick F, Ray AS, Miller MD.** 2006. In vitro evaluation of the anti-HIV activity and metabolic interactions of tenofovir and emtricitabine. Antivir. Ther. **11**:377–384.
5. **Feng JY, Ly JK, Myrick F, Goodman D, White KL, Svarovskaia ES, Borroto-Esoda K, Miller MD.** 2009. The triple combination of tenofovir, emtricitabine and efavirenz shows synergistic anti-HIV-1 activity in vitro: a mechanism of action study. Retrovirology **6**:44. doi:10.1186/1742-4690-6-44.
6. **Kawamoto A, Kodama E, Sarafianos SG, Sakagami Y, Kohgo S, Kitano K, Ashida N, Iwai Y, Hayakawa H, Nakata H, Mitsuya H, Arnold E, Matsuoka M.** 2008. 2′-Deoxy-4′-C-ethynyl-2-halo-adenosines active against drug-resistant human immunodeficiency virus type 1 variants. Int. J. Biochem. Cell Biol. **40**:2410–2420.
7. **Michailidis E, Marchand B, Kodama EN, Singh K, Matsuoka M, Kirby KA, Ryan EM, Sawani AM, Nagy E, Ashida N, Mitsuya H, Parniak MA, Sarafianos SG.** 2009. Mechanism of inhibition of HIV-1 reverse transcriptase by 4′-ethynyl-2-fluoro-2′-deoxyadenosine triphosphate, a translocation-defective reverse transcriptase inhibitor. J. Biol. Chem. **284**:35681–35691.
8. **Kirby KA, Singh K, Michailidis E, Marchand B, Kodama EN, Ashida N, Mitsuya H, Parniak MA, Sarafianos SG.** 2011. The sugar ring conformation of 4′-ethynyl-2-fluoro-2′-deoxyadenosine and its recognition by the polymerase active site of HIV reverse transcriptase. Cell Mol. Biol. **57**:40–46.
9. **Murphey-Corb M, Rajakumar P, Michael H, Nyaundi J, Didier PJ, Reeve AB, Mitsuya H, Sarafianos SG, Parniak MA.** 2012. Response of simian immunodeficiency virus to the novel nucleoside reverse transcriptase inhibitor 4′-ethynyl-2-fluoro-2′-deoxyadenosine in vitro and in vivo. Antimicrob. Agents Chemother. **56**:4707–4712.
10. **Hattori S, Ide K, Nakata H, Harada H, Suzu S, Ashida N, Kohgo S, Hayakawa H, Mitsuya H, Okada S.** 2009. Potent activity of a nucleoside reverse transcriptase inhibitor, 4′-ethynyl-2-fluoro-2′-deoxyadenosine, against human immunodeficiency virus type 1 infection in a model using human peripheral blood mononuclear cell-transplanted NOD/SCID Janus kinase 3 knockout mice. Antimicrob. Agents Chemother. **53**:3887–3893.
11. **Prichard MN, Prichard LE, Shipman C, Jr.** 1993. Strategic design and three-dimensional analysis of antiviral drug combinations. Antimicrob. Agents Chemother. **37**:540–545.
12. **Prichard MN, Shipman C, Jr.** 1990. A three-dimensional model to analyze drug-drug interactions. Antiviral Res. **14**:181–205.
13. **Chou TC, Talalay P.** 1984. Quantitative analysis of dose-effect relationships: the combined effects of multiple drugs or enzyme inhibitors. Adv. Enzyme Regul. **22**:27–55.
14. **Pirrone V, Thakkar N, Jacobson JM, Wigdahl B, Krebs FC.** 2011. Combinatorial approaches to the prevention and treatment of HIV-1 infection. Antimicrob. Agents Chemother. **55**:1831–1842.
15. **Chang CN, Skalski V, Zhou JH, Cheng YC.** 1992. Biochemical pharmacology of (+)- and (−)-2′,3′-dideoxy-3′-thiacytidine as anti-hepatitis B virus agents. J. Biol. Chem. **267**:22414–22420.
16. **Sabini E, Hazra S, Konrad M, Lavie A.** 2007. Nonenantioselectivity property of human deoxycytidine kinase explained by structures of the enzyme in complex with L- and D-nucleosides. J. Med. Chem. **50**:3004–3014.
17. **Hachiya A, Kodama EN, Schuckmann MM, Kirby KA, Michailidis E, Sakagami Y, Oka S, Singh K, Sarafianos SG.** 2011. K70Q adds high-level tenofovir resistance to "Q151M complex" HIV reverse transcriptase through the enhanced discrimination mechanism. PLoS One **6**:e16242. doi:10.1371/journal.pone.0016242.
18. **Kirby KA, Marchand B, Ong YT, Ndongwe TP, Hachiya A, Michailidis E, Leslie MD, Sietsema DV, Fetterly TL, Dorst CA, Singh K, Wang Z, Parniak MA, Sarafianos SG.** 2012. Structural and inhibition studies of the RNase H function of xenotropic murine leukemia virus-related virus reverse transcriptase. Antimicrob. Agents Chemother. **56**:2048–2061.
19. **Nakata H, Amano M, Koh Y, Kodama E, Yang G, Bailey CM, Kohgo S, Hayakawa H, Matsuoka M, Anderson KS, Cheng YC, Mitsuya H.** 2007. Activity against human immunodeficiency virus type 1, intracellular metabolism, and effects on human DNA polymerases of 4′-ethynyl-2-fluoro-2′-deoxyadenosine. Antimicrob. Agents Chemother. **51**:2701–2708.
20. **Abdool Karim Q, Abdool Karim SS, Frohlich JA, Grobler AC, Baxter C, Mansoor LE, Kharsany AB, Sibeko S, Mlisana KP, Omar Z, Gengiah TN, Maarschalk S, Arulappan N, Mlotshwa M, Morris L, Taylor D.** 2010. Effectiveness and safety of tenofovir gel, an antiretroviral microbicide, for the prevention of HIV infection in women. Science **329**:1168–1174.
21. **Grant RM, Lama JR, Anderson PL, McMahan V, Liu AY, Vargas L, Goicochea P, Casapia M, Guanira-Carranza JV, Ramirez-Cardich ME, Montoya-Herrera O, Fernandez T, Veloso VG, Buchbinder SP, Chariyalertsak S, Schechter M, Bekker LG, Mayer KH, Kallas EG, Amico KR, Mulligan K, Bushman LR, Hance RJ, Ganoza C, Defechereux P, Postle B, Wang F, McConnell JJ, Zheng JH, Lee J, Rooney JF, Jaffe HS, Martinez AI, Burns DN, Glidden DV.** 2010. Preexposure chemoprophylaxis for HIV prevention in men who have sex with men. N. Engl. J. Med. **363**:2587–2599.
22. **Richman D, Rosenthal AS, Skoog M, Eckner RJ, Chou TC, Sabo JP, Merluzzi VJ.** 1991. BI-RG-587 is active against zidovudine-resistant human immunodeficiency virus type 1 and synergistic with zidovudine. Antimicrob. Agents Chemother. **35**:305–308.
23. **Brennan TM, Taylor DL, Bridges CG, Leyda JP, Tyms AS.** 1995. The inhibition of human immunodeficiency virus type 1 in vitro by a non-nucleoside reverse transcriptase inhibitor MKC-442, alone and in combination with other anti-HIV compounds. Antiviral Res. **26**:173–187.
24. **King RW, Klabe RM, Reid CD, Erickson-Viitanen SK.** 2002. Potency of nonnucleoside reverse transcriptase inhibitors (NNRTIs) used in

combination with other human immunodeficiency virus NNRTIs, NRTIs, or protease inhibitors. Antimicrob. Agents Chemother. **46:** 1640–1646.

25. **Maga G, Hubscher U, Pregnolato M, Ubiali D, Gosselin G, Spadari S.** 2001. Potentiation of inhibition of wild-type and mutant human immunodeficiency virus type 1 reverse transcriptases by combinations of nonnucleoside inhibitors and D- and L-(beta)-dideoxynucleoside triphosphate analogs. Antimicrob. Agents Chemother. **45:**1192–1200.
26. **Borkow G, Arion D, Wainberg MA, Parniak MA.** 1999. The thiocarboxanilide nonnucleoside inhibitor UC781 restores antiviral activity of 3′-azido-3′-deoxythymidine (AZT) against AZT-resistant human immunodeficiency virus type 1. Antimicrob. Agents Chemother. **43:**259–263.
27. **Odriozola L, Cruchaga C, Andreola M, Dolle V, Nguyen CH, Tarrago-Litvak L, Perez-Mediavilla A, Martinez-Irujo JJ.** 2003. Non-nucleoside inhibitors of HIV-1 reverse transcriptase inhibit phosphorolysis and resensitize the 3′-azido-3′-deoxythymidine (AZT)-resistant polymerase to AZT-5′-triphosphate. J. Biol. Chem. **278:**42710–42716.
28. **Cruchaga C, Odriozola L, Andreola M, Tarrago-Litvak L, Martinez-Irujo JJ.** 2005. Inhibition of phosphorolysis catalyzed by HIV-1 reverse transcriptase is responsible for the synergy found in combinations of 3′-azido-3′-deoxythymidine with nonnucleoside inhibitors. Biochemistry **44:**3535–3546.
29. **Basavapathruni A, Bailey CM, Anderson KS.** 2004. Defining a molecular mechanism of synergy between nucleoside and nonnucleoside AIDS drugs. J. Biol. Chem. **279:**6221–6224.
30. **Radzio J, Sluis-Cremer N.** 2008. Efavirenz accelerates HIV-1 reverse transcriptase ribonuclease H cleavage, leading to diminished zidovudine excision. Mol. Pharmacol. **73:**601–606.
31. **Shaw-Reid CA, Feuston B, Munshi V, Getty K, Krueger J, Hazuda DJ, Parniak MA, Miller MD, Lewis D.** 2005. Dissecting the effects of DNA polymerase and ribonuclease H inhibitor combinations on HIV-1 reverse-transcriptase activities. Biochemistry **44:**1595–1606.
32. **Parikh UM, Koontz DL, Chu CK, Schinazi RF, Mellors JW.** 2005. In vitro activity of structurally diverse nucleoside analogs against human immunodeficiency virus type 1 with the K65R mutation in reverse transcriptase. Antimicrob. Agents Chemother. **49:**1139–1144.

AAC
Journals.ASM.org

Effects of Substitutions at the 4′ and 2 Positions on the Bioactivity of 4′-Ethynyl-2-Fluoro-2′-Deoxyadenosine

Karen A. Kirby,[a,b] Eleftherios Michailidis,[a,b] Tracy L. Fetterly,[a,b] Musetta A. Steinbach,[a,b] Kamalendra Singh,[a,b] Bruno Marchand,[a,b] Maxwell D. Leslie,[a,b] Ariel N. Hagedorn,[a,b] Eiichi N. Kodama,[c] Victor E. Marquez,[d] Stephen H. Hughes,[e] Hiroaki Mitsuya,[f,g] Michael A. Parniak,[h] Stefan G. Sarafianos[a,b,i]

Christopher Bond Life Sciences Center, University of Missouri, Columbia, Missouri, USA[a]; Department of Molecular Microbiology & Immunology, University of Missouri School of Medicine, Columbia, Missouri, USA[b]; Division of Emerging Infectious Diseases, Tohoku University School of Medicine, Sendai, Japan[c]; Chemical Biology Laboratory, Center for Cancer Research, National Cancer Institute-Frederick, Frederick, Maryland, USA[d]; HIV Drug Resistance Program, National Cancer Institute-Frederick, Frederick, Maryland, USA[e]; Department of Internal Medicine, Kumamoto University School of Medicine, Kumamoto Japan[f]; Experimental Retrovirology Section, HIV/AIDS Malignancy Branch, National Institutes of Health, Bethesda, Maryland, USA[g]; Department of Microbiology & Molecular Genetics, University of Pittsburgh School of Medicine, Pittsburgh, Pennsylvania, USA[h]; Department of Biochemistry, University of Missouri, Columbia, Missouri, USA[i]

Nucleos(t)ide reverse transcriptase inhibitors (NRTIs) form the backbone of most anti-HIV therapies. We have shown that 4′-ethynyl-2-fluoro-2′-deoxyadenosine (EFdA) is a highly effective NRTI; however, the reasons for the potent antiviral activity of EFdA are not well understood. Here, we use a combination of structural, computational, and biochemical approaches to examine how substitutions in the sugar or adenine rings affect the incorporation of dA-based NRTIs like EFdA into DNA by HIV RT and their susceptibility to deamination by adenosine deaminase (ADA). Nuclear magnetic resonance (NMR) spectroscopy studies of 4′-substituted NRTIs show that ethynyl or cyano groups stabilize the sugar ring in the C-2′-exo/C-3′-endo (north) conformation. Steady-state kinetic analysis of the incorporation of 4′-substituted NRTIs by RT reveals a correlation between the north conformation of the NRTI sugar ring and efficiency of incorporation into the nascent DNA strand. Structural analysis and the kinetics of deamination by ADA demonstrate that 4′-ethynyl and cyano substitutions decrease the susceptibility of adenosine-based compounds to ADA through steric interactions at the active site. However, the major determinant for decreased susceptibility to ADA is the 2-halo substitution, which alters the pK_a of N1 on the adenine base. These results provide insight into how NRTI structural attributes affect their antiviral activities through their interactions with the RT and ADA active sites.

There are 10 nucleos(t)ide reverse transcriptase inhibitors (NRTIs) that are currently approved for the treatment of human immunodeficiency virus type 1 (HIV-1) infections (1–5). Several more nucleoside analog drugs are approved or being studied for the treatment of viruses, such as herpes simplex virus (HSV), hepatitis C virus (HCV), and hepatitis B virus (HBV), or as anticancer agents (6–10). NRTIs are among the most effective anti-HIV drugs. All approved anti-HIV NRTIs lack a 3′-hydroxyl moiety and, thus, act as chain terminators following their incorporation by the viral reverse transcriptase (RT) into the nascent DNA chain. However, the absence of a 3′-OH, while essential for the inhibition of DNA synthesis, also imparts detrimental properties to these inhibitors, including reduced intracellular phosphorylation to the active triphosphate form and reduced RT binding affinity (11). Prolonged exposure to NRTI-based treatments causes mitochondrial toxicity (12–14) and leads to the development of NRTI resistance mutations (15–18), giving rise to complications in the treatment of HIV-infected patients.

Ideally, an NRTI should have a strong binding affinity for the RT target, a high barrier for the development of resistance, and low toxicity. We have reported that a series of 4′-substituted nucleosides in which the 3′-OH is retained has exceptional inhibitory activity against HIV-1 RT (19). Among these compounds, 4′-ethynyl-2-fluoro-2′-deoxyadenosine (EFdA) is a highly active RT inhibitor that prevents translocation of the nucleic acid from the nucleotide-binding or pretranslocation site to the primer-binding or posttranslocation site on RT following its incorporation at the 3′ primer terminus (20). Depending on the DNA template sequence, EFdA can also act (albeit less frequently) as a delayed chain terminator, incorporating one incoming deoxynucleoside triphosphate (dNTP) before DNA synthesis is blocked (20). We previously showed that EFdA inhibits HIV replication in peripheral blood mononuclear cells (PBMCs) with a 50% effective concentration (EC_{50}) of 0.05 nM (20). Additionally, EFdA effectively inhibits the replication of many common drug-resistant strains of HIV, including strains that carry a substitution of R for K at position 65 (K65R) (a 0.2-fold change in EC_{50}) (21, 22), N348I (a 0.9-fold change in 50% inhibitory concentration [IC_{50}]) (23), the excision-enhancing mutations M41L and T215Y (a 1.5-fold change in EC_{50}) (21), and multidrug resistance Q151M complex mutations (A62V/V75I/F77L/F116Y/Q151M) (a 0.7-fold change in EC_{50}) (21). EFdA is also able to inhibit HIV containing the M184V drug resistance mutation (with an EC_{50} of 8.3 nM, or a 7.5-fold change) (21, 24). EFdA is generally a poor substrate for human DNA polymerases in *in vitro* experiments (IC_{50}s of >100 μM for polymerase α and β and 10 μM for polymerase γ; EFdA-triphosphate [EFdA-TP] is incorporated by polymerase γ 4,300-

Received 6 August 2013 Returned for modification 10 September 2013
Accepted 29 September 2013
Published ahead of print 7 October 2013
Address correspondence to Stefan G. Sarafianos, sarafianoss@missouri.edu.
Supplemental material for this article may be found at http://dx.doi.org/10.1128/AAC.01703-13.

doi:10.1128/AAC.01703-13

fold less efficiently than dATP) and, thus, has a low potential for cytotoxicity (25, 26). Because the 50% cytotoxic concentration (CC_{50}) for EFdA is more than 10 μM in MT4 cells or PBMCs, the selectivity of the compound is high. Moreover, in studies with simian immunodeficiency virus (SIV)-infected macaques, no signs of clinical or pathological drug toxicity were observed after 6 months of continuous EFdA monotherapy (24). These data suggest that EFdA is a strong candidate for further development as a therapeutic agent.

The EC_{50s} of NRTIs are also affected by cellular uptake, activation to the active metabolite by host kinases, and catabolism by cellular enzymes. Previous studies have shown that EFdA has a favorable cellular uptake profile and is efficiently phosphorylated to EFdA-TP (25). Additional reported data strongly suggest that, in cells, EFdA is phosphorylated to EFdA-monophosphate (EFdA-MP) by deoxycytidine kinase (dCK) (21). The molecular details of the efficiency and specificity of this process are being investigated in separate studies. The enzyme adenosine deaminase (ADA), which is present at high concentrations in human serum, is involved in the catabolism of dA and its analogs (27, 28). ADA is responsible for the deamination of adenosine or deoxyadenosine analogs to inosine- or deoxyinosine-based products (27, 29–33) and can therefore affect the activation pathway and intracellular concentration of dA-based compounds. For example, ADA converts dideoxyadenosine (ddA) to ddI, leading to a different and indirect activation pathway for ddA (28, 34, 35). Thus, it is important to study the interaction of dA-based compounds, such as EFdA, with ADA to gain insights into their catabolism and subsequent activation pathways.

We have also previously reported that small changes in the chemical composition of dA analogs can have a pronounced effect on their antiviral potency. These changes can be complex, because they can have different and at times opposing effects on the recognition of NRTIs by the RT target and the various enzymes involved in activation and catabolism. For example, the presence of fluorine or another halogen at the 2 position on the adenine base of 4′-substituted dA analogs significantly enhanced their antiviral activity (21). Similarly, the nature of the 4′ substitutions on the deoxyribose ring also affected the EC_{50}s of dA-based compounds against both wild-type (WT) and NRTI-resistant HIV-1 variants (19).

Additionally, changes in the conformation of the sugar ring and in the nature of the nucleobase can affect the biological activity of NRTIs. In solution, the structure of the deoxyribose ring of nucleosides exists in a dynamic equilibrium between the C-2′-exo/C-3′-endo (north) and C-2′-endo/C-3′-exo (south) conformations. We have previously shown that EFdA exists primarily in the north conformation (36) and that HIV-1 RT prefers the NRTI or incoming dNTP sugar ring in the north conformation for optimal binding (37–40). In contrast, host cell kinases appear to prefer the sugar ring in the south conformation; compounds that favor the north conformation are generally phosphorylated inefficiently (41, 42). Sugar ring conformation has also been reported to play an important role in ADA recognition; the enzyme has been reported to deaminate nucleosides biased toward the north conformation up to 65-fold faster than those biased toward the south conformation (43–46). Additionally, 2-fluoro-2′-deoxyadenosine (FdA) analogs are somewhat resistant to ADA-mediated catabolism due to the electron withdrawing properties of the 2-fluoro group (47, 48), and we have previously reported that EFdA is poorly deaminated by ADA because of the 2-fluoro group (21). However, the effects of specific 4′ substitutions on sugar ring conformation and how these substitutions would affect the recognition of the compounds by HIV RT and ADA have not been determined.

In the present work, we carried out a series of structural, computational, and biochemical studies using a variety of 2- and 4′-substituted dA and dT analogs (Fig. 1) to understand the specific effects of these different substitutions on sugar ring conformation, recognition by HIV RT, and deamination by ADA. Our data show how the 2-fluoro and 4′-ethynyl moieties affect the antiviral potential of NRTIs and help determine the basis for the favorable inhibitory profile of EFdA.

MATERIALS AND METHODS

Chemicals. Compounds dA, FdA, and dT (compound abbreviations are defined and their numbers specified in Results) were purchased from Sigma-Aldrich (St. Louis, MO). Triphosphate forms of dA and dT were purchased from Fermentas (Glen Burnie, MD). Compounds 13 to 14 and the triphosphate forms of compounds 10, 11, 13, and 14 were synthesized by Marquez and colleagues as previously described (49, 50). ADA (bovine intestine, EC 3.5.4.4) was purchased from Calbiochem (San Diego, CA). Deuterated dimethyl sulfoxide (DMSO-D_6) was purchased from Cambridge Isotope Laboratories, Inc. (Andover, MA).

Nucleic acid substrates. DNA oligomers were synthesized by Integrated DNA Technologies (Coralville, IA). In steady-state kinetics assays of dATP and dATP analogs, a 26-nucleotide-long DNA template (T_{d26A}; CCA TAG ATA GCA TTG GTG CTC GAA CA) was used. In steady-state kinetics assays of dTTP and dTTP analogs, a 26-nucleotide-long template (T_{d26T}; CCA TAG TAA GCA TTG GTG CTC GAA CA) was used. An 18-nucleotide-long 5′-fluorescently labeled DNA primer (P_{d18}; TGT TCG AGC ACC AAT GCT) was annealed to both T_{d26A} and T_{d26T}.

NMR spectroscopy. One-dimensional ^{1}H nuclear magnetic resonance (NMR) spectra were collected in 10°C increments from 20 to 50°C on a Bruker Avance DRX500 operating at 500 MHz and equipped with a 5-mm HCN cryoprobe, as previously described (36). Samples were dissolved in DMSO-D_6 to give concentrations of 2 to 4 mM. Spectra were processed with resolution enhancement using negative line broadening (lb = −0.3). Coupling constants were analyzed by spectral simulation using SpinWorks 3.0 (Kirk Marat, University of Manitoba, Winnipeg, Canada). Simulations were performed for the spin systems on the deoxyribose ring only. The root mean square (RMS) deviations of calculated and experimental coupling constants for all compounds were <0.15 Hz.

Pseudorotational analysis. The sugar ring conformations of the nucleoside analogs were determined using the program PSEUROT 6.3 (DOS version, purchased from Cornelis Altona, University of Leiden, Leiden, The Netherlands) as previously described (36). PSEUROT assumes a two-state approximation (equilibrium between north and south conformations) and utilizes a generalized Karplus equation combined with a nonlinear Newton-Raphson minimization process to examine the conformational flexibility of five-membered rings (51). An iterative methodology was used to determine the optimal pseudorotational parameters P_N and P_S (pseudorotational phase angle [P] for the north [N]or south [S] conformation) and $\phi_m(N)$ and $\phi_m(S)$ (degree of maximum ring pucker [ϕ_m] for the north or south conformation), in which some of these parameters were fixed during refinement in order to constrain the values within the range commonly observed for nucleosides (average observed, $\phi_m = 39°$).

Molecular orbital calculations. In order to determine the role of molecular orbitals in the stability of the north and south sugar ring conformations of EFdA, we carried out molecular orbital calculations using semiempirical quantum chemical methods. All quantum chemical calculations were performed by the density functional theory (DFT) method using the B3LYP approach with 6-31G** basis sets. The quantum chem-

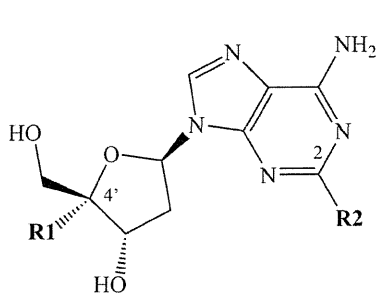

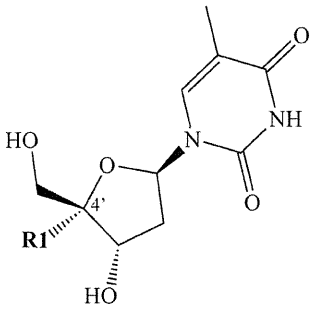

Deoxyadenosine Analogs

Sugar R1	Base R2	Compound Abbreviation
−H	−H	dA (**1**)
−H	−F	FdA (**2**)
−C≡CH	−H	EdA (**3**)
−C≡CH	$-NH_2$	EdDAP (**4**)
−C≡CH	−F	EFdA (**5**)
−C≡CH	−Cl	ECldA (**6**)
−C≡N	−H	CNdA (**7**)
−C≡N	$-NH_2$	CNdDAP (**8**)
−C≡N	−F	CNFdA (**9**)
$-CH_3$	−H	MedA (**10**)*
$-CH_2CH_3$	−H	EtdA (**11**)*

Thymidine Analogs

Sugar R1	Compound Abbreviation
−H	dT (**12**)
$-CH_3$	MedT (**13**)
$-CH_2CH_3$	EtdT (**14**)

FIG 1 Deoxyadenosine and thymidine analogs used in the study. *, only the triphosphate forms of these compounds were used in this study.

istry program Jaguar (Schrödinger, Inc., NY) was used for all computations. The structures of north and south conformations of EFdA were completely optimized by restricting the position of the 3′-C either in the north or south conformation. To obtain insight into the interaction of the lone pairs of the O4 and 3′-O atoms with the antibonding (π^*) orbitals of the 4′-ethynyl group of EFdA, the natural bond orbitals (NBOs), natural (semi-)localized molecular orbitals (NLMOs), and canonical molecular orbitals (CMOs) were computed using the program NBO (version 5.0) (52, 53).

HIV-1 RT steady-state kinetic assays. The steady-state kinetic parameters, K_m and k_{cat}, for incorporation of dNTPs and dNTP analogs were determined using single-nucleotide incorporation in gel-based assays under saturating substrate conditions. The reactions were carried out in 50 mM Tris-HCl, pH 7.8, 50 mM NaCl, 6 mM $MgCl_2$, 100 nM T_{d26A}/P_{d18} for dATP analogs, 100 nM T_{d26T}/P_{d18} for dTTP analogs, and 10 nM RT in a final volume of 20 μl and stopped at the reaction times of 1.5 to 3 min. The products were resolved on 15% polyacrylamide 7 M urea gels, and the gels were scanned with a Typhoon FLA 9000 phosphorimager (GE Healthcare). The bands were quantified using Multi Gauge software (FujiFilm). K_m and k_{cat} values were determined graphically using the Michaelis-Menten equation in GraphPad Prism 4 (GraphPad Software, Inc.).

ADA kinetic assays. The deamination rates of dA (compound 1), EdA (compound 3), and CNdA (compound 7) were determined by following the disappearance of the substrate on a BioTek Synergy HT spectrophotometer at 265 nm in 100-μl solutions at 25°C with 0.1 M phosphate, pH 7.4. A change in molar extinction coefficients for all of the deaminated products was assumed to be $\Delta\varepsilon = -7{,}900$ for all dA analogs (45). For each assay, the substrate concentrations varied between 15 μM and 240 μM. Absorbance was measured every 20 s. Three determinations were made for each analog. K_m and k_{cat} for each compound were determined using Michaelis-Menten plots (GraphPad Prism 4).

Because the reactions of ADA with FdA (compound 2), EFdA (compound 5), ECldA (compound 6), and CNFdA (compound 9) were very slow under these conditions, a high-pressure liquid chromatography (HPLC) method was used to observe the hydrolytic deamination of these compounds (54). In order to separate the substrate and product of the reaction, an elution gradient was developed using various combinations of 0.1 M phosphate, pH 7.4, and methanol. The following gradient was run on an Agilent 1100 series HPLC system: 7% methanol for 3 min, 14% methanol for 2 min, 21% methanol for 2 min, 28% methanol for 2 min, 35% methanol for 5 min, and 7% methanol for the final 2 min, returning the conditions to the original state. The gradient ran for a total of 16 min at a flow rate of 1 ml/min and an injection volume of 60 μl. The method ran at room temperature, and the absorbance was measured at a wavelength of 260 nm. The solvents used for the HPLC gradient were vacuum filtered prior to use.

Kinetic measurements were made using dA (compound 1), FdA (compound 2), EdA (compound 3), EFdA (compound 5), ECldA (compound 6), CNdA (compound 7), and CNFdA (compound 9) as ADA substrates. The reactions were carried out in 0.1 M phosphate buffer, pH 7.4. The FdA (compound 2) and EFdA (compound 5) analogs were tested using concentrations ranging from 10 μM to 9 mM. Compounds dA (compound 1), EdA (compound 3), ECldA (compound 6), CNdA (compound 7), and CNFdA (compound 9) were tested at 500 μM. Reactions were started by the addition of 2.4 mU ADA. The reactions were run for 45 min at 25°C before being terminated by the addition of perchlorate at 0.3

TABLE 1 Summary of pseudorotational analysis of the sugar ring of deoxyadenosine and thymidine analogs

Compound (no.)	P_N (°)	P_S (°)	$\phi_m(N)$ (°)	$\phi_m(S)$ (°)	% North	RMS error (Hz)[a]
Deoxyadenosine analogs						
dA (1)[b]	18.7	169.1	39.0[c]	31.1	23	0.03
FdA (2)	3.4	169.1	38.7	29.2	24	0.01
EdA (3)	37.3	152.1	39.0[c]	39.0[c]	64	0.40
EdDAP (4)	39.7	152.1	39.0[c]	39.0[c]	63	0.49
EFdA (5)[b]	38.7	146.5	39.0[c]	39.0[c]	75	0.20
EClda (6)	38.4	148.0	39.0[c]	39.0[c]	73	0.21
CNdA (7)	47.8	152.8	38.0[c]	38.0[c]	61	0.12
CNdDAP (8)	45.0	154.0[c]	37.2	38.0[c]	56	0.12
CNFdA (9)	41.6	154.2	38.0[c]	38.0[c]	59	0.23
Thymidine analogs						
MedT (13)	24.3	132.5	38.0[c]	31.5	43	0.05
EtdT (14)	23.3	150.3	38.0[c]	30.2	39	0.18

[a] Root mean square deviation between experimental and calculated coupling constants.
[b] Values previously reported (36).
[c] Value fixed during calculations.

M final concentration. Denatured protein was removed from the reaction mixture by using centrifugation at 10,000 rpm for 5 min to pellet the protein. The clear supernatant was then removed, and the final pH was adjusted to 7.4 by adding Na_2CO_3 to reach a final concentration of 2.5 mM (54).

Structural analysis of predicted EFdA interactions at the active site of ADA. Structural analysis of EFdA interactions at the ADA active site were carried out using the coordinates of human ADA in complex with dA obtained from the RCSB Protein Data Bank (PDB ID 3IAR). EFdA was drawn and minimized using the ChemBioDraw Ultra 13.0 and ChemBio3D Ultra 13.0 software from the ChemBioOffice Suite (PerkinElmer, Waltham, MA). Using the Coot model building software package (55), the structure of EFdA was superposed to the dA molecule, followed by the removal of dA.

RESULTS

Effect of 4′ substitutions on the structure of dA and dT analogs. To evaluate the structural effects of the 4′ substitutions on the sugar ring conformations of the dA and dT analogs, we collected one-dimensional ^{1}H NMR spectra over a range of physiologically relevant temperatures for the following compounds: 2′-deoxyadenosine (dA, compound 1), 2-fluoro-2′-deoxyadenosine (FdA, compound 2), 4′-ethynyl-2′-deoxyadenosine (EdA, compound 3), 4′-ethynyl-2′-deoxyribofuranosyl-2,6-diaminopurine (EdDAP, also known as ENdA, compound 4), 4′-ethynyl-2-fluoro-2′-deoxyadenosine (EFdA, compound 5), 4′-ethynyl-2-chloro-2′-deoxyadenosine (EClda, compound 6), 4′-cyano-2′-deoxyadenosine (CNdA, compound 7), 4′-cyano-2′-deoxyribofuranosyl-2,6-diaminopurine (CNdDAP, compound 8), 4′-cyano-2-fluoro-2′-deoxyadenosine (CNFdA, compound 9), thymidine (dT, compound 12), 4′-methyl-thymidine (MedT, compound 13), and 4′-ethyl-thymidine (EtdT, compound 14) (Fig. 1) (36). Resolving the coupling constants between most of the hydrogen atoms on the deoxyribose ring required spectral simulation (see Table S1 in the supplemental material). The coupling constants determined from each spectrum were used to calculate the structural parameters of the deoxyribose ring of each compound. The changes in the value of each coupling constant with temperature were used to calculate the pseudorotational phase angle, P, and the degree of maximum ring pucker, ϕ_m, for the C-2′-exo/C-3′-endo (north or *N*) and C-2′-endo/C-3′-exo (south or *S*) sugar ring conformations (see Fig. S1 in the supplemental material) of the nucleoside analogs in this study.

The pseudorotational parameters listed in Table 1 were calculated using PSEUROT 6.3 as described in Materials and Methods and our previous report (36). The value of P_N for each of the 4′-ethynyl- or cyano-substituted deoxyadenosine compounds 3 to 9 (P_N = 37.3 to 47.8°) lies in the northern hemisphere of the pseudorotational pathway (P_N = 0 to 90°), although these values are higher than what is typically observed for most nucleosides (P_N = 0 to 36°) (see Fig. S1 in the supplemental material). These values correspond to a conformation between $_4T^3$ (P_N = 36°) and $_4$E or 4′-exo (P_N = 54°) in the pseudorotational pathway (see Fig. S1) (56). A similar conformation was determined by Siddiqui et al. from the crystal structure of 4′-ethynyl-2′,3′-dideoxycytidine (P_N = 43.5°) (57). The P_N values of the 4′-cyano-substituted compounds 7 to 9 (P_N = 41.6 to 47.8°) are slightly higher than those observed for the 4′-ethynyl-substituted compounds 3 to 6 (P_N = 37.3 to 39.7°). The values of P_N for the 4′-methyl- and 4′-ethyl-substituted thymidine compounds (P_N = 24.3° and 23.3°, respectively) were also in the northern hemisphere but were much lower than those observed for the 4′-ethynyl and 4′-cyano analogs. These values correspond to a conformation between ^{3}E or 3′-endo (P_N = 18°) and $_4T^3$ (P_N = 36°) in the pseudorotational pathway (see Fig. S1) (56).

The pseudorotational values determined for dA (compound 1) are in agreement with previous reports, demonstrating that dA strongly prefers the south conformation (36, 45). Comparison of the conformational parameters of dA (compound 1) versus EdA (compound 3) (23% versus 64% north) and FdA (compound 2) versus EFdA (compound 5) (24% versus 75% north) showed that the 4′-ethynyl strongly favors the north conformation of the sugar (Table 1 and Fig. 2). Comparison of dA (compound 1) versus CNdA (compound 7) (23% versus 61% north) and FdA (compound 2) versus CNFdA (compound 9) (24% versus 59% north) showed that the 4′-cyano also has a large effect on sugar conformation, albeit smaller than that of the 4′-ethynyl group (% north in EdA [compound 3] > % north in CNdA [compound 7] and % north in EFdA [compound 5] > % north in CNFdA [compound 9]) (Table 1).

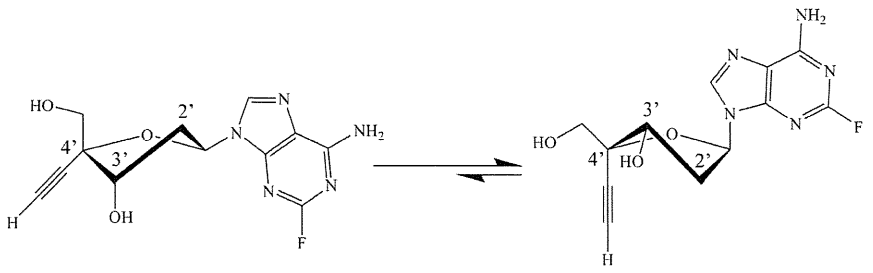

FIG 2 Dynamic equilibrium between the south and north sugar ring conformations of 4′-ethynyl-substituted compounds in solution (EFdA is shown). Natural deoxynucleoside substrates favor the south conformation.

Evaluation of the conformational parameters of the thymidine analogs dT (compound 12), MedT (compound 13), and EtdT (compound 14) demonstrated that 4′-methyl and ethyl substitutions have smaller effects on the sugar ring conformation than 4′-ethynyl and cyano groups. Although we were unable to accurately determine the coupling constants for dT (compound 12) due to overlap of one of the 2′-H signals with the DMSO solvent peak, it has previously been determined that the deoxyribose ring of dT favors the south conformation, which is similar to dA (56, 58). 4′-Methyl and 4′-ethyl substitutions shift the equilibrium toward the north conformation relative to the equilibrium of thymidine (43% and 39% north, respectively), but this effect is smaller than that of a 4′-ethynyl or 4′-cyano substitution in dA analogs (64% and 61% north compared to 23% in dA) (Table 1).

Hence, the 4′-ethynyl substitution imparts the largest effect on the conformation of the deoxyribose ring, followed by the 4′-cyano, the 4′-methyl, and the 4′-ethyl groups.

Effect of 2 position substitutions on the structure of dA analogs. Using the same method, we also assessed the effect of substitutions at the 2 position of the adenine base on the structure of dA analogs. Evaluation of the conformation parameters of dA (compound 1) versus FdA (compound 2) showed that substitutions at the 2 position of the adenine base have little to no effect on sugar ring conformation. Similarly, comparisons of the 4′-ethynyl-substituted EdA (compound 3), EdDAP (compound 4), EFdA (compound 5), and EClda (compound 6) showed that the 2-fluoro and 2-chloro substitutions have only a modest effect on the sugar ring conformation (Table 1). Finally, comparisons of CNdA (compound 7), CNdDAP (compound 8), and CNFdA (compound 9) also confirmed that 2-fluoro and 2-amino substitutions on the adenine ring have no significant impact on the sugar ring conformation (61%, 56%, and 59% north, respectively) (Table 1).

Molecular orbital calculations. Potential stabilizing orbital interactions can occur between a lone pair of electrons in a p-like fully occupied orbital and an unoccupied antibonding orbital, allowing the delocalization of electrons and, thus, increasing molecular stability. To determine whether there are any favorable orbital interactions in the north or south sugar ring conformations of EFdA that could stabilize one conformation versus the other, we carried out quantum chemical computations to assess the orbital interactions of the lone pairs of the O4 and 3′-O atoms with the antibonding (π^*) orbitals of the 4′-ethynyl moiety. We first determined the electronic composition of natural bond orbitals (NBOs) and their contribution in the formation of natural (semi-)localized molecular orbitals (NLMOs). The NBOs are localized orbitals that describe the Lewis-like molecular bonding pattern of electron pairs (59). The NLMOs have been described as semilocalized alternatives to canonical molecular orbitals (CMOs) for representing the electron pairs of MO-type wave functions. Each NLMO consists of a parent NBO (strictly localized) and associated delocalizations needed to describe the density of a full electron pair (59). The NBOs were used to compute CMOs. Both the north and south sugar ring conformations of EFdA have 375 NBOs (which include bonding orbitals, core orbitals, lone pairs, antibonding orbitals, and Rydberg orbitals), 76 NLMOs, and 375 CMOs. To assess the orbital interaction involving the lone pairs of O4 and 3′-O and the antibonding orbitals (π^*) of the 4′-ethynyl group, we examined the second-order perturbative estimates of donor-acceptor (bond-antibond) NBO interactions for both north and south conformations. These estimates provide the measure of delocalization due to the interaction of the O4 or 3′-O lone pair with the π^* antibonding orbital of the 4′-ethynyl group. Table 2 summarizes the energy of the donor-acceptor NBO interactions. These results suggest that the interaction of the lone pairs of the O4 and 3′-O atoms with the antibonding orbitals of the 4′-ethynyl moiety contributes to the greater stabilization energy (~2-fold) of the north conformation. Further NBO analyses show the reduced occupancy of the O4 and 3′-O lone pairs (10% and 6%, respectively) and the remote interaction of both lone pairs with the antibonding NBOs of the 4′-C≡C in the north conformation. In the south conformation, the O4 and 3′-O lone pairs have a reduced occupancy of 7% and 4%, respectively, and only the O4 lone pair has a remote interaction with the antibonding NBOs of the 4′-C≡C. The NLMO analyses of the north conformation showed that the lone pairs of both O4 and 3′-O

TABLE 2 Summary of molecular orbital calculations[a]

NBO donor (LP)	NBO acceptor (π^*)	Interaction energy (kcal/mol) for EFdA conformation	
		North	South
O4	4′-C≡C	1.63	1.25
3′-O	4′-C≡C	0.71	0.0
Total energy		2.34	1.25

[a] LP, lone pair; π^*, antibonding orbital.

TABLE 3 Steady-state kinetic parameters for incorporation of the triphosphate forms of the 4′-substituted compounds by HIV-1 RT

dNTP	K_m (μM)[a]	k_{cat} (min^{-1})[a]	k_{cat}/K_m (min^{-1} · μM^{-1})	Fold change in incorporation efficiency[b]
dATP	2.35 ± 0.06	0.66 ± 0.13	0.3	1
EFdA-TP	0.27 ± 0.01	3.47 ± 0.04	12.9	45.9
EdDAP-TP	0.15 ± 0.01	2.55 ± 0.10	17.0	60.7
MedA-TP	0.29 ± 0.01	1.24 ± 0.05	4.3	15.3
EtdA-TP	0.88 ± 0.19	3.41 ± 0.12	3.9	13.9
dTTP	0.60 ± 0.01	1.04 ± 0.12	1.7	1
MedT-TP	0.68 ± 0.22	1.58 ± 0.15	2.3	1.3
EtdT-TP	2.00 ± 0.22	1.44 ± 0.20	0.7	0.4

[a] Values are means ± standard deviations of two independent experiments and were determined from the Michaelis-Menten equation using GraphPad Prism 4.
[b] Fold change in incorporation efficiency is the ratio of the incorporation efficiency (k_{cat}/K_m) of NRTI-TP over that of dATP or dTTP [$(k_{cat}/K_m)_{NRTI\text{-}TP}/(k_{cat}/K_m)_{dATP}$ or $(k_{cat}/K_m)_{NRTI\text{-}TP}/(k_{cat}/K_m)_{dTTP}$].

atoms are delocalized into the vicinal region (C-5′ and 4′-C≡C, ~5% and 2%, respectively). The delocalization of the O4 lone pair in the vicinal C-5′ and 4′-C≡C groups for the south conformation is significantly less than ~1%, and there is almost no delocalization of the 3′-O lone pair in the C-5′ and 4′-C≡C vicinity. Taken together, these data suggest (i) that the north sugar ring conformation is more stable than the south and (ii) that the north conformation is stabilized by the interactions of the O4 and 3′-O lone pairs with the antibonding orbitals of the 4′-ethynyl group.

Effect of 4′ substitutions on the ability of dA and dT analogs to block reverse transcription *in vitro*. In order to assess the effect of various 4′ substitutions on the ability of dA and dT analogs to block reverse transcription *in vitro*, we tested the triphosphate forms of compounds 1, 4, 5, and 10 to 14 for their ability to block DNA synthesis by HIV-1 RT (Table 3). Additional previously published *in vitro* and cell-based inhibition data for dA and dT analogs are summarized in Table S2 in the supplemental material. Remarkably, almost all 4′-substituted analogs are excellent substrates of HIV-1 RT and are incorporated even more efficiently than the canonical substrate (higher k_{cat}/K_m). Specifically, the 4′-ethynyl substitution resulted in the highest efficiencies of inhibitor incorporation (EdDAP-TP and EFdA-TP have 60- and 45-fold higher k_{cat}/K_m than dATP). The higher efficiency appears to be the result of both increased catalytic turnover rate (k_{cat}) and decreased K_m (Table 3). Notably, the enhancement in incorporation efficiency *in vitro* appears to be more pronounced for the dA than for the dT analogs (Table 3). Moreover, 4′-ethynyl dA analogs are 3 to 4 times more efficiently incorporated by HIV-1 RT than 4′-methyl compounds. Inhibitors containing a 4′-ethyl modification are the least efficiently incorporated by HIV-1 RT.

Effect of 4′ substitutions on susceptibility to ADA. Bovine ADA was chosen to study the hydrolytic deamination of compounds 1 to 7 and 9 because it is readily available and because it is highly similar to human ADA (91% overall and 100% active-site sequence identity) (60, 61), allowing us to use the biochemical data to infer what would happen with the human enzyme. We found that 4′ substitutions decreased the ability of ADA to use these nucleosides as substrates, primarily due to an increase in K_m (Table 4). The 4′-ethynyl and 4′-cyano groups have similar effects on ADA catabolism.

TABLE 4 Summary of steady-state kinetic data for the deamination of dA, EdA, and CNdA by ADA[a]

Compound (no.)	Mean K_m ± SD (μM)	k_{cat} (s^{-1})	k_{cat}/K_m (s^{-1} · μM^{-1})
dA (1)	42.6 ± 15.0	13.5	0.32
EdA (3)	145.9 ± 37.6	11.3	0.08
CNdA (7)	156.9 ± 84.2	8.9	0.06

[a] Data were determined spectrophotometrically.

Effect of 2 position substitutions on susceptibility to ADA. Because the 2 position-substituted compounds were refractory to hydrolytic deamination by ADA, we were unable to obtain reliable kinetic measurements using the spectrophotometric assay. In order to at least obtain a relative order of susceptibility to ADA, we used an HPLC-based assay (54), which allowed long incubation times and a determination of the amount of product from the slow hydrolytic deamination of compounds 2, 5, 6, and 9 by ADA. These experiments showed that incubation of 500 μM substrate for 45 min resulted in 15% conversion of FdA (compound 2), 1.3% of EFdA (compound 5), 2.8% of ECldA (compound 6), and <1% of CNFdA (compound 9) (Fig. 3). These data suggest that the 2-halo combined with 4′ substitutions resulted in significantly decreased susceptibility of the dA compounds to ADA and that the decreasing order of stability was CNFdA (compound 9) > EFdA (compound 5) > ECldA (compound 6) > FdA (compound 2). This is consistent with our previous report that EFdA is not efficiently deaminated by ADA (21).

Structural analysis of predicted EFdA interactions at the ADA active site. Using the crystal structure coordinates of human ADA, we looked for potential interactions between the active-site residues and the modeled EFdA that could lead to decreased susceptibility of this inhibitor to ADA. As shown in Fig. 4, the placement of EFdA at the expected position of a substrate would result in unfavorable steric interactions between the 4′-ethynyl group of EFdA and the sulfur and ε-carbon of Met155 (d = 2.2 and 2.0 Å, respectively). These potential steric effects could contribute to a lower binding affinity for EdA than for dA, consistent with an ~3.5-fold difference in the corresponding K_m values ($K_{m\text{-EdA}}$ = 146 μM versus $K_{m\text{-dA}}$ = 43 μM), which is the primary contributing factor in the observed decrease in the catalytic efficiency of ADA when EdA is the substrate.

DISCUSSION

We have previously demonstrated that EFdA is more potent against WT and drug-resistant HIV strains than other approved NRTIs (19–24) in both biochemical and virological assays and that it has low cytotoxicity (24–26). This suggests that EFdA not only has a high affinity toward HIV-1 RT but is also likely to be efficiently activated by host kinases (21, 25) and is relatively stable in cells (21). In fact, a favorable NRTI EC_{50} depends on multiple desirable attributes that include (i) a strong binding affinity of the active metabolite for the RT target, (ii) efficient cellular uptake and activation by host kinases, (iii) an ability to withstand deactivation by cellular enzymes, (iv) a high barrier to resistance, and (v) low cytotoxicity. The present study investigates how different substitutions on the sugar ring and adenine base contribute to the structural features of NRTIs and the effects of these features on the first three of the factors listed above.

Sugar puckering affects several aspects of the activity of EFdA

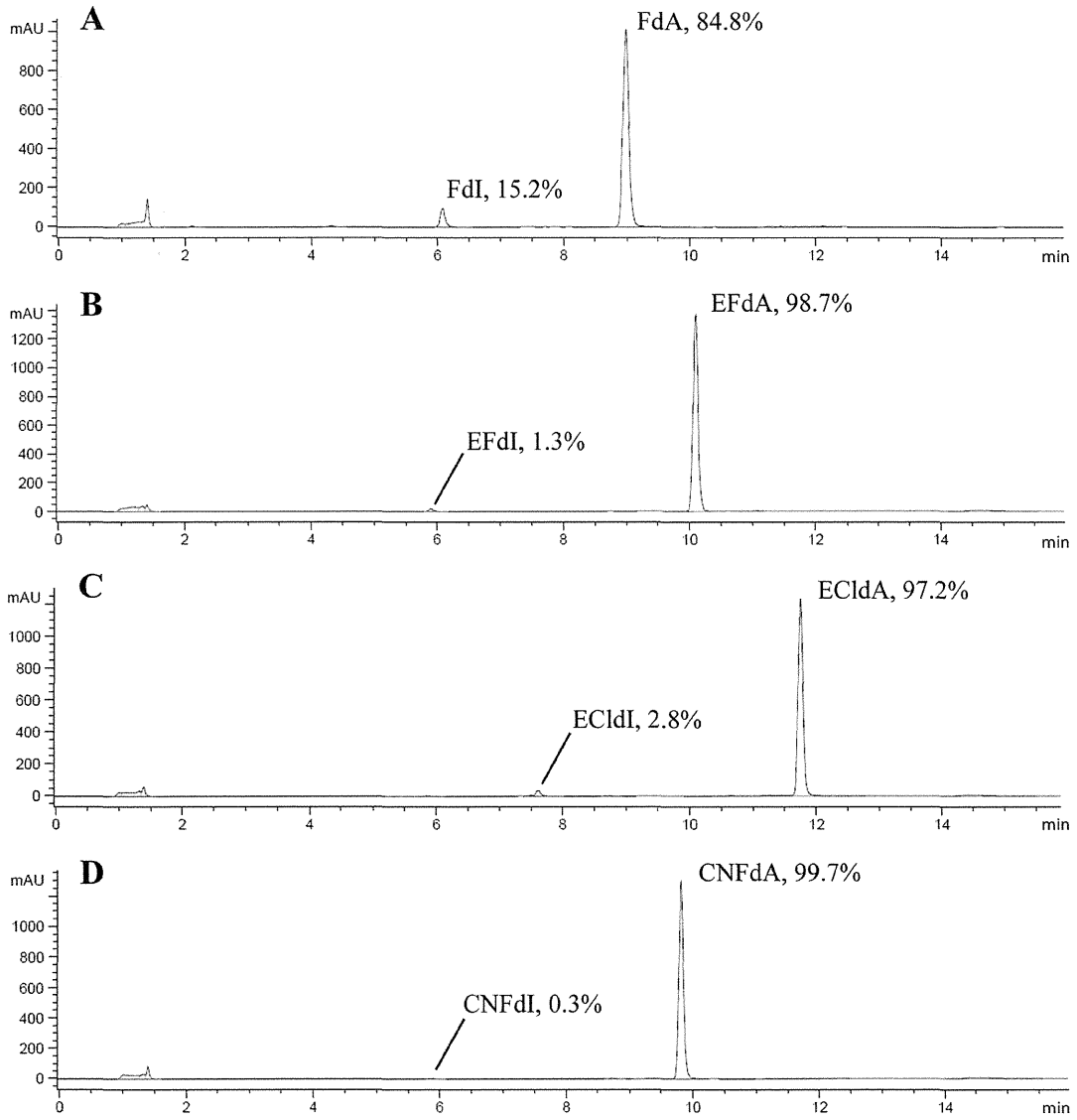

FIG 3 HPLC data taken after reaction of dA analogs (500 μM) with ADA for 45 min (260-nm signal is shown in blue). FdA (A), EFdA (B), ECldA (C), and CNFdA (D) were converted to the corresponding deoxyinosine (dI) forms to different extents. Percentages of dA-based reactant and dI-based product were calculated based on peak areas.

by influencing its interactions with HIV RT, dCK, and ADA. We have previously proposed that the extent to which an NRTI can exist in the north conformation affects its potency. In that respect, we have shown (Marquez and colleagues) that HIV-1 RT prefers as a substrate a version of zidovudine-triphosphate (AZT-TP) that is locked in the north rather than in the south conformation (38), suggesting that the HIV-1 RT active site prefers nucleosides or their analogs in the north conformation. Our NMR data and molecular orbital calculations demonstrate that the 4′-ethynyl substitution causes the sugar ring conformation of EFdA to be primarily in the north conformation. This causes it (and presumably the structure of its active metabolite EFdA-TP) to reside in a favorable conformation for binding at the polymerase active site of HIV-1 RT (36). This hypothesis is further supported by our steady-state kinetic assays and a previous report of *in vitro* HIV RT inhibition by EFdA-TP (20).

For a nucleoside analog to be a potent inhibitor of HIV replication, it must be converted to the triphosphate form in cells. The nucleoside substrate type or sugar ring conformation can affect the ability of cellular kinases to activate nucleoside analogs. The type of nucleoside substrate can determine which kinase will carry out the initial phosphorylation step. For example, dCK preferentially phosphorylates dC, dA, and dG analogs (62, 63), whereas thymidine kinase 1 phosphorylates dT analogs (64). Hence, the differences in phosphorylation efficiency of various NRTIs likely depend, at least in part, on the fact that different kinases are used to convert the various analogs to the active metabolite (65). Moreover, the activation of NRTIs involves multiple enzymes whose specificity may also impact the efficiency of activation. For example, AZT-MP is not phosphorylated efficiently to AZT-diphosphate (AZT-DP) by thymidylate kinase, and this is the rate-limiting step in AZT-TP formation (25, 66).

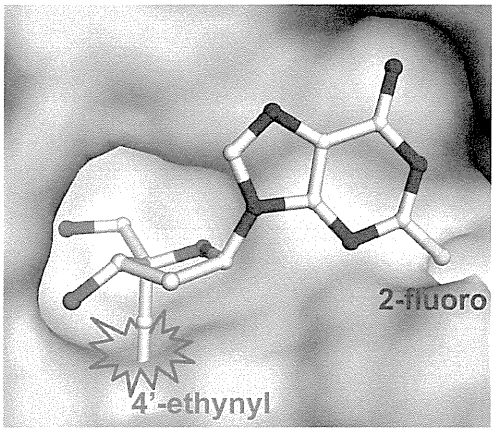

FIG 4 Structural analysis of the predicted effect of the 4′-ethynyl group of EFdA (yellow sticks) on interactions with the binding pocket of ADA (gray surface). When EFdA binds in a manner similar to that of other substrates, the 4′-ethynyl group may clash with the sulfur and ε-carbon atoms of Met155 in ADA. The figure was made using the PyMOL molecular graphics software package (http://www.pymol.org/).

The sugar ring conformation can also affect the ability of host kinases to activate nucleoside analogs. For example, dCK is known to bind its natural nucleoside substrates in the south conformation (41, 42). Interestingly, although the EFdA sugar ring favors the north conformation, it appears to be phosphorylated efficiently by dCK in cells (25). This suggests that other structural features of EFdA may contribute to its efficient phosphorylation, such as the 4′-ethynyl, the 2-fluoro, or both. In fact, it has been previously reported that a 2-fluoro substitution on dA decreases the K_m value 33-fold compared to that of dA, making FdA a very efficient substrate for dCK (63). Ongoing structural studies of EFdA in complex with dCK should reveal the basis of efficient activation of EFdA by dCK.

The EC_{50} of NRTIs can also be affected by catabolizing enzymes. For example, ADA can deaminate dA-based nucleosides and change the pathway and efficiency of their activation. The activity of ADA is affected by the structural determinants of its substrates. While we have previously demonstrated (Marquez and colleagues) that this enzyme efficiently deaminates nucleoside analogs in the north conformation (43–46), the kinetic analysis of ADA that we report here shows that the presence of a substituent at the 2 position of the adenine base makes these derivatives poor substrates for ADA. These results agree with previous studies reporting that 2-halo-substituted compounds are not efficiently deaminated by ADA (29, 31–33).

The mechanism by which 2-halo substitutions affect ADA activity does not appear to involve steric interactions in the ADA binding pocket (Fig. 4). This suggests that they decrease susceptibility through electronic rather than steric effects. The electronic effect of 2-fluoro can be explained in terms of changes in pK_a and charge distribution on the adenine base. The deamination mechanism by ADA involves an addition-elimination reaction on the substrate to form an inosine-based product (Fig. 5A). The first step involves electrophilic attack to protonate the N1 position of the purine ring, followed by nucleophilic attack at the C-6 position of the ring to form a tetrahedral intermediate (67–70). The introduction of an electronegative fluorine atom at the 2 position has been reported to dramatically lower the pK_a of the N1 atom of adenosine-based compounds (more than 100-fold) (Fig. 5B) (71). This is the result of the highly electronegative fluorine atom increasing the positive charge at the C-2 position (C-2 ∂^+, F ∂^-), which would raise the energy barrier of N1 protonation. Hence, the N1 protonation step becomes the rate-limiting step of the hydrolytic deamination reaction, thus reducing the yield of the 2-fluoro deoxyinosine product (Fig. 3). The presence of a 2-amino instead of a 2-halo substitution has a different effect on the mechanism and efficiency of the deamination reaction. In the case of EdDAP, a resonance effect caused by the 2-amino substitution would distribute the positive charge of the protonated N1 to all neighboring nitrogen atoms. Hence, differences in the deamina-

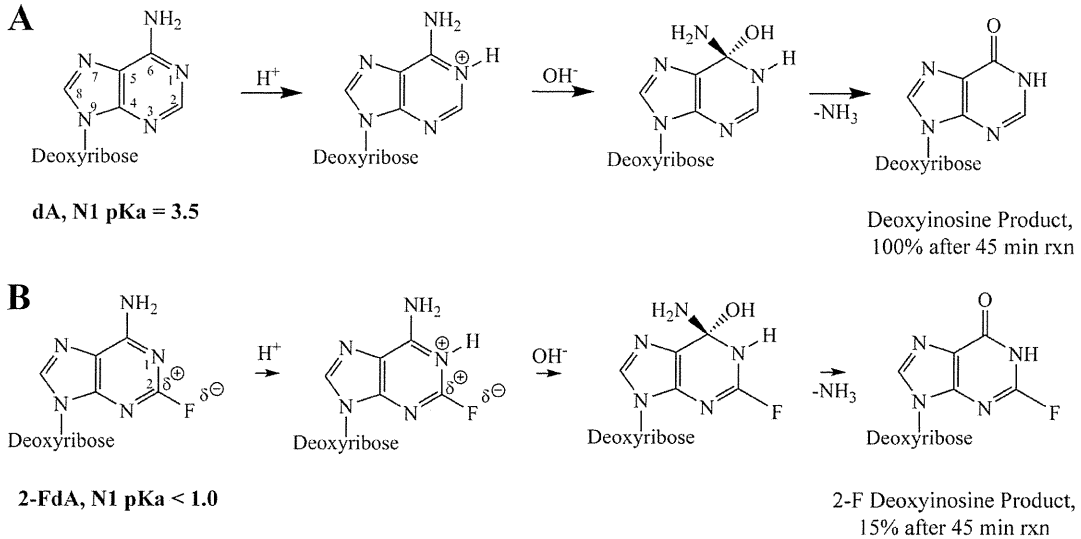

FIG 5 Reaction mechanism of hydrolytic deamination of dA (A) and FdA (B) by adenosine deaminase (67–70). The electronegative 2-fluoro group causes a dramatic decrease in pK_a at the N1 position (71), resulting in a high-energy barrier for the N1 protonation step of the reaction. rxn, reaction.